

Nb₃Sn Development and Characterization

**Carmine SENATORE, Gianmarco BOVONE, Francesco LONARDO, Romain BABOUCHE,
Marco ACOSTA, Florin BUTA**

Simon HOPKINS, Thierry BOUTBOUL

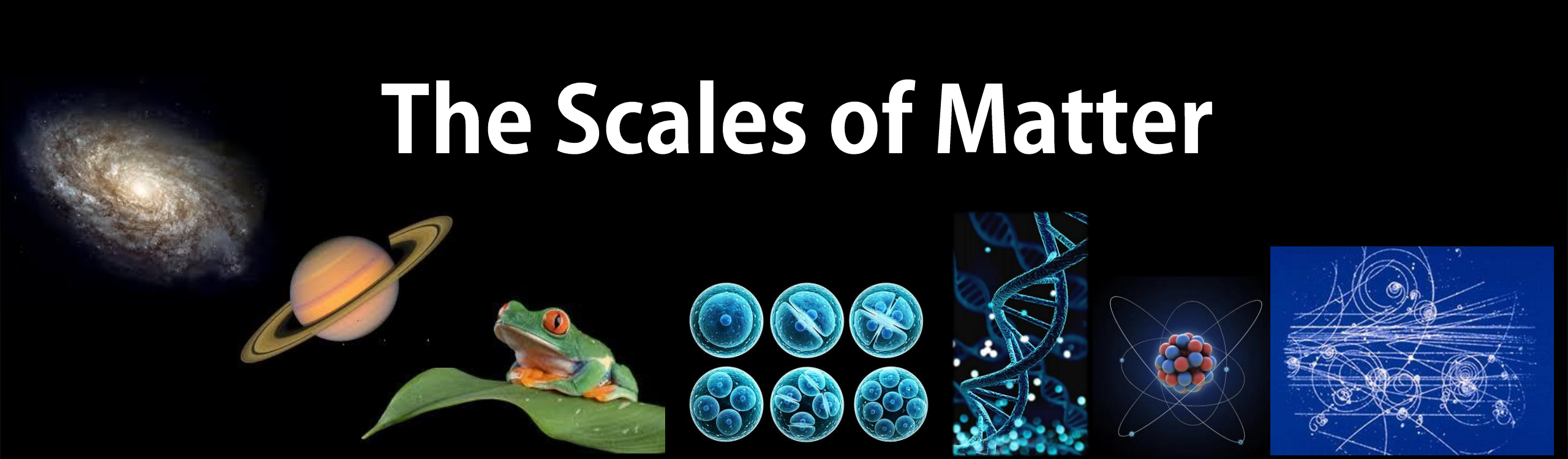
Outline

- **Towards application-ready Nb₃Sn wires with enhanced performance**
 - **Internal Oxidation** and **APCs**: material properties and practical implementation
- **Electromechanical properties of state-of-the-art Nb₃Sn wires**
 - Effects of the **longitudinal strain** on magnet design **margins**
 - Influence of the **wire layout** on the **transverse stress tolerance**
- **Summary and conclusions**

Outline

- **Towards application-ready Nb₃Sn wires with enhanced performance**
 - **Internal Oxidation** and **APCs**: material properties and practical implementation
- Electromechanical properties of state-of-the-art Nb₃Sn wires
 - Effects of the **longitudinal strain** on magnet design **margins**
 - Influence of the **wire layout** on the **transverse stress tolerance**
- Summary and conclusions

The Scales of Matter



10^{24} m

10^7 m

10^0 m

10^{-5} m

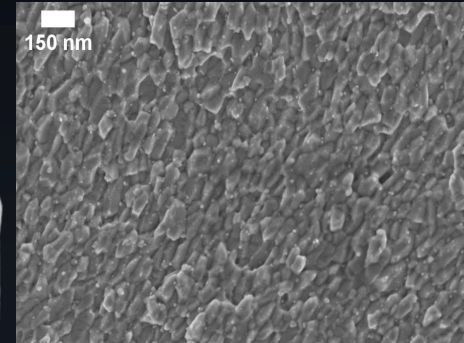
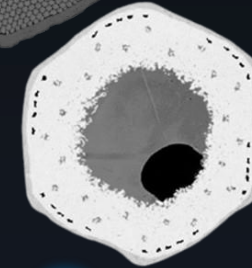
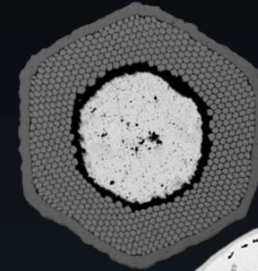
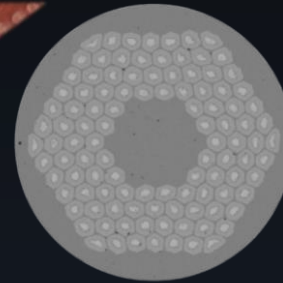
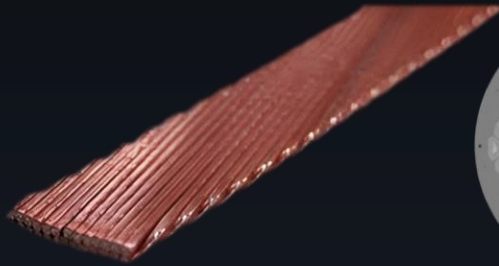
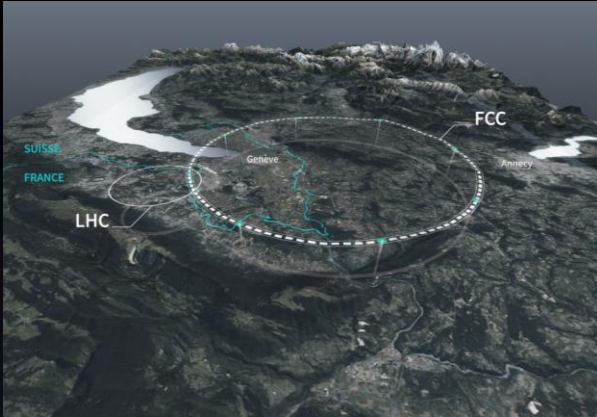
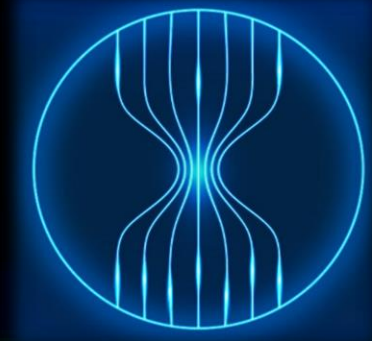
10^{-9} m

10^{-15} m

10^{-19} m



The Scales of HFM



10^5 m

10^1 m

10^{-2} m

10^{-3} m

10^{-5} m

10^{-8} m

The Scales of R&D at

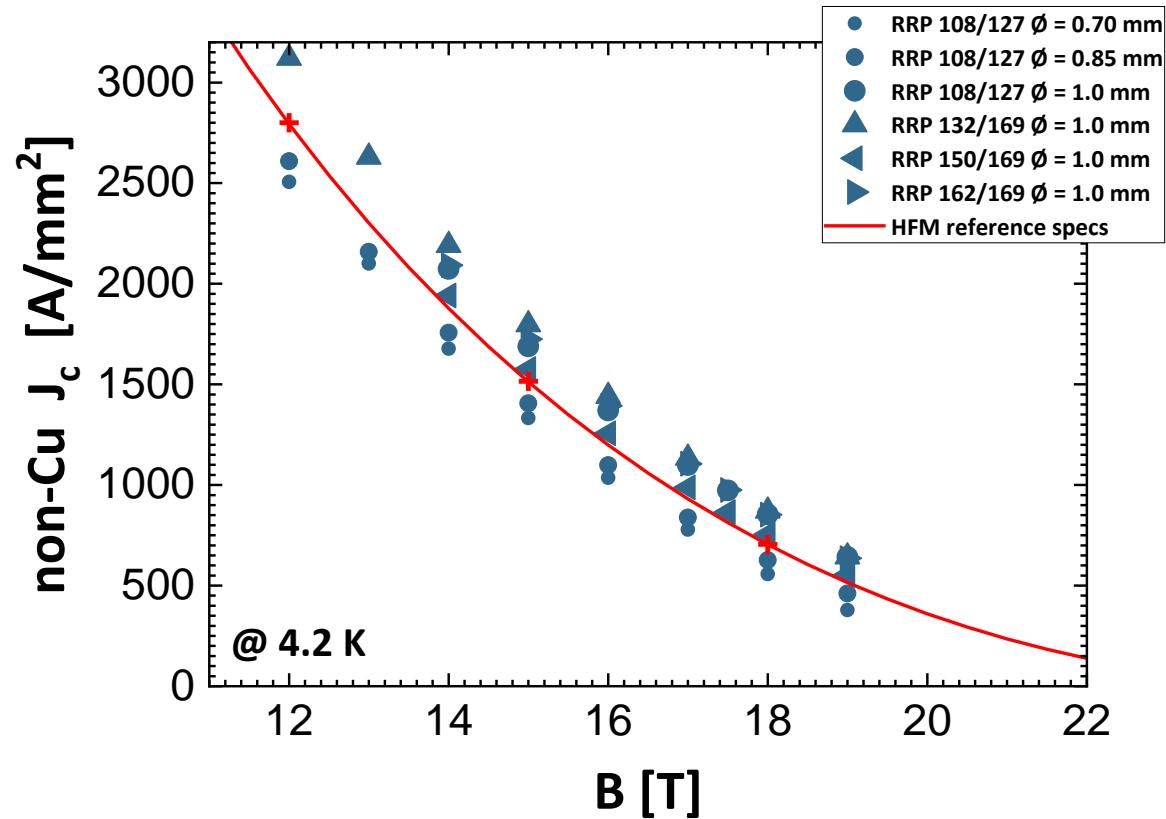


UNIVERSITÉ
DE GENÈVE

FACULTÉ DES SCIENCES

Performance of state-of-the-art wires

HL-LHC & HFM RRP wires and HFM specs



R. Babouche, HFM Forum (2025)

URL: indico.cern.ch/event/1543973/

Subelement composition to maximize non-Cu J_c

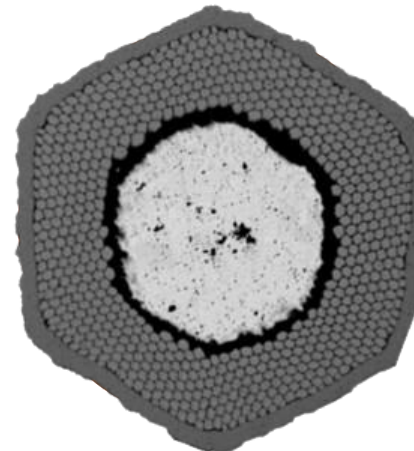


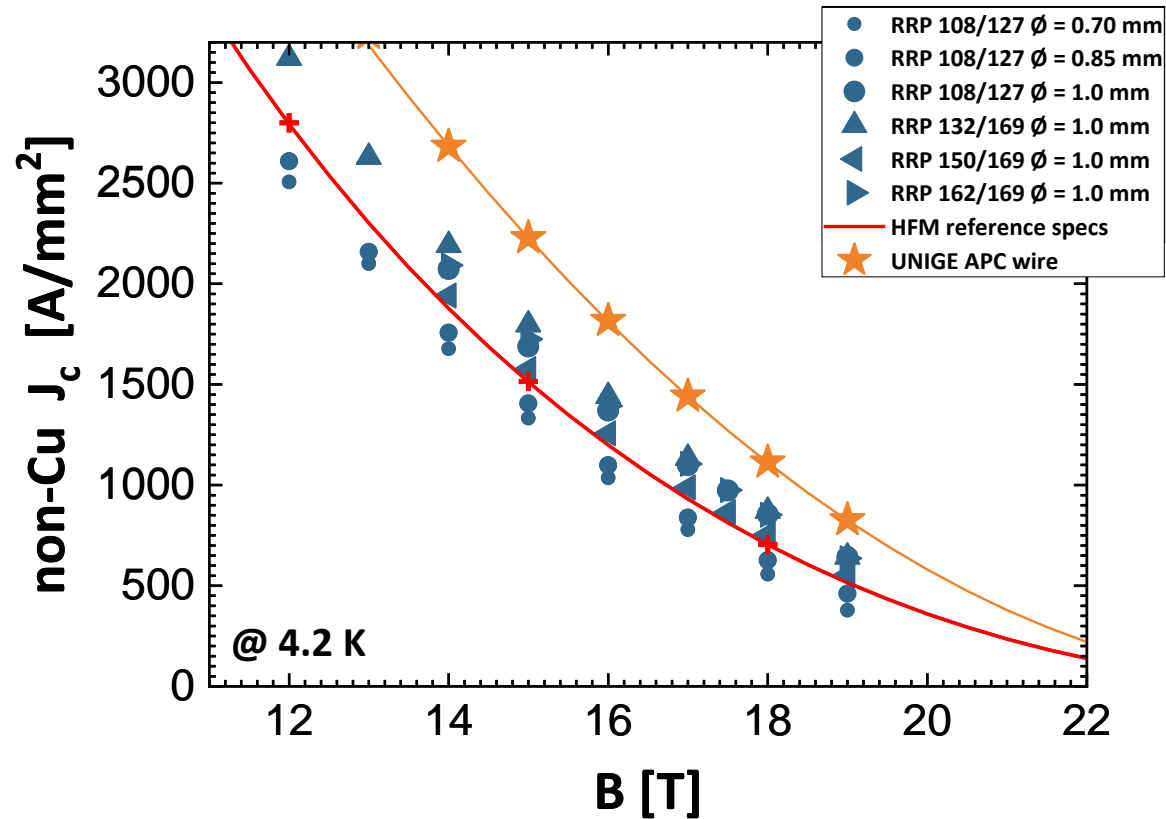
TABLE 1

Parameter	Range	Preferred Range
Total Nb content	50-65% of Non-Cu	55-60% of Non-Cu
Sn wt % / ((Sn wt % + Cu wt %) within the diffusion barrier	45-65%	50-60%
Local Area Ratio	0.10-0.30	0.15-0.25
Nb to Sn atomic ratio	2.7-3.7	3.1-3.6
Nb filament diameter	0.5-7 microns	1-5 microns
Nb diff. barrier thickness	0.8-11 microns	1.5-8 microns
Nb barrier fraction of Nb	20-50%	25-35%

M. Field, J. Parrell, Y. Zhang, [Patent US 7,368,021 B2](#)

Performance of state-of-the-art wires and Improvement Prospects with Internal Oxidation

HL-LHC & HFM RRP wires and HFM specs



R. Babouche, HFM Forum (2025)

URL: indico.cern.ch/event/1543973/

Internal Oxidation – APC – Nb-Ta-Hf alloy

non-Cu J_c calculated for a HL-LHC wire layout from the measured layer J_c . – non-Cu $J_c = 0.6$ layer J_c . Data from:

Bovone *et al.*, Supercond. Sci. Tech. **36** (2023) 095018

DOI: [10.1088/1361-6668/aced25](https://doi.org/10.1088/1361-6668/aced25)

Subelement composition to maximize non-Cu J_c

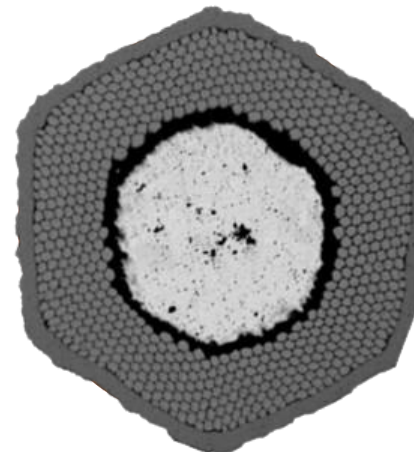
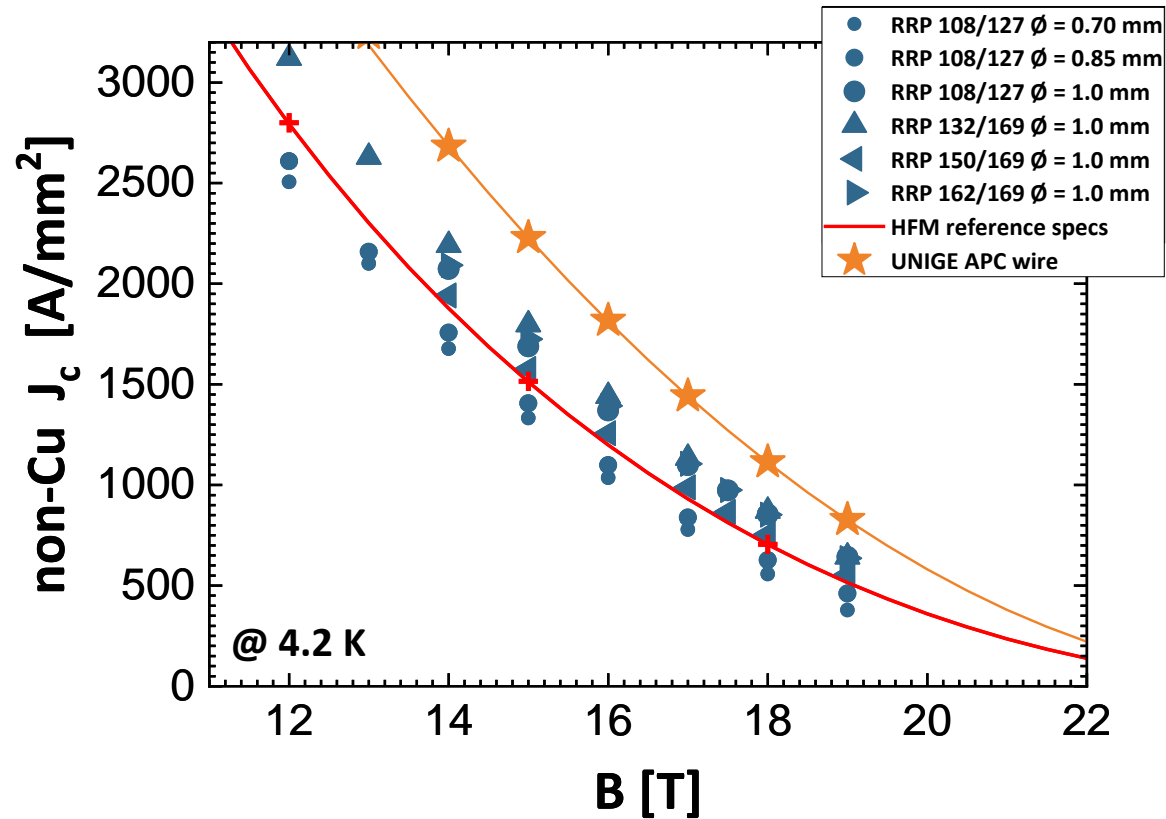


TABLE 1

Parameter	Range	Preferred Range
Total Nb content	50-65% of Non-Cu	55-60% of Non-Cu
Sn wt %/(Sn wt % + Cu wt %) within the diffusion barrier	45-65%	50-60%
Local Area Ratio	0.10-0.30	0.15-0.25
Nb to Sn atomic ratio	2.7-3.7	3.1-3.6
Nb filament diameter	0.5-7 microns	1-5 microns
Nb diff. barrier thickness	0.8-11 microns	1.5-8 microns
Nb barrier fraction of Nb	20-50%	25-35%

M. Field, J. Parrell, Y. Zhang, [Patent US 7,368,021 B2](https://patent.uspto.gov/patent/US7368021B2)

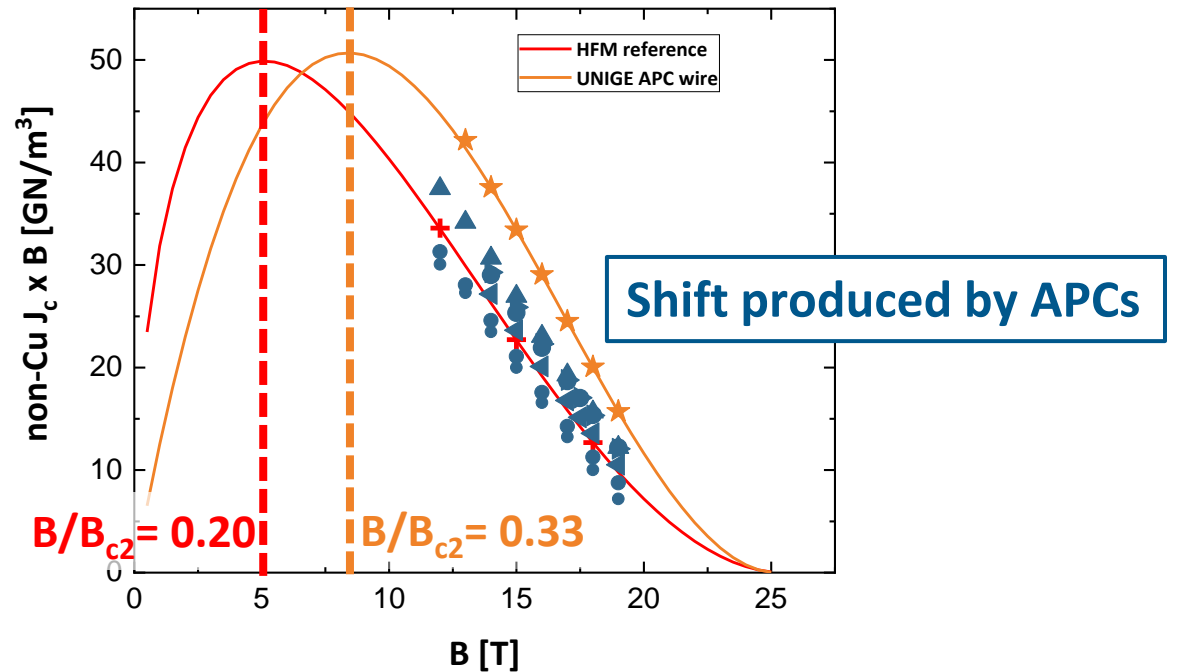
Performance of state-of-the-art wires and Improvement Prospects HL-LHC & HFM RRP wires and HFM specs with Internal Oxidation



R. Babouche, HFM Forum (2025)
URL: indico.cern.ch/event/1543973/

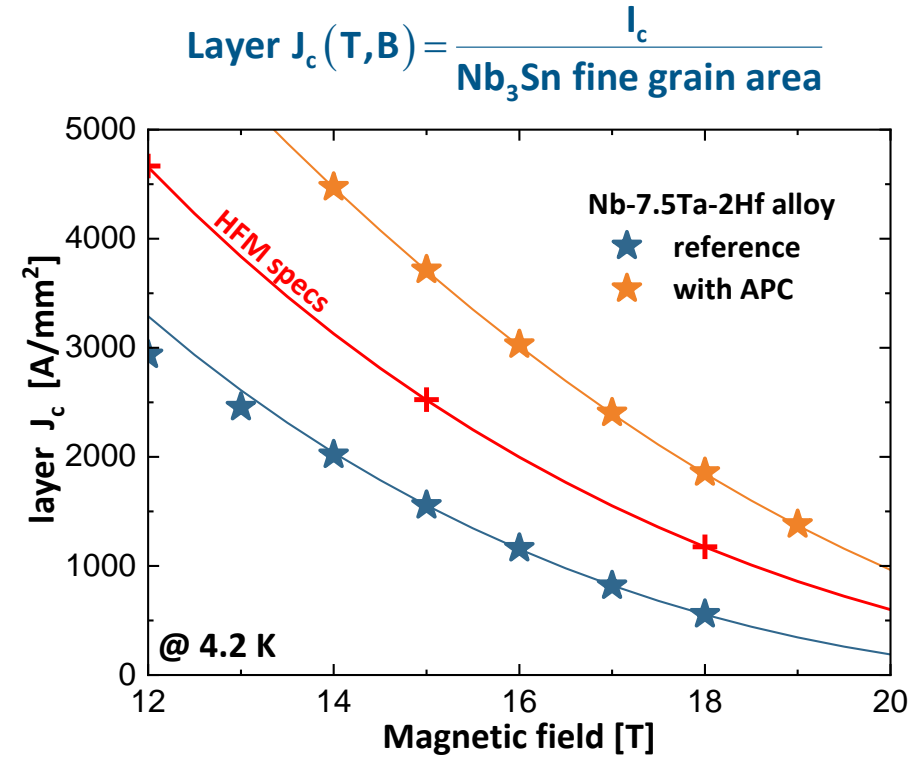
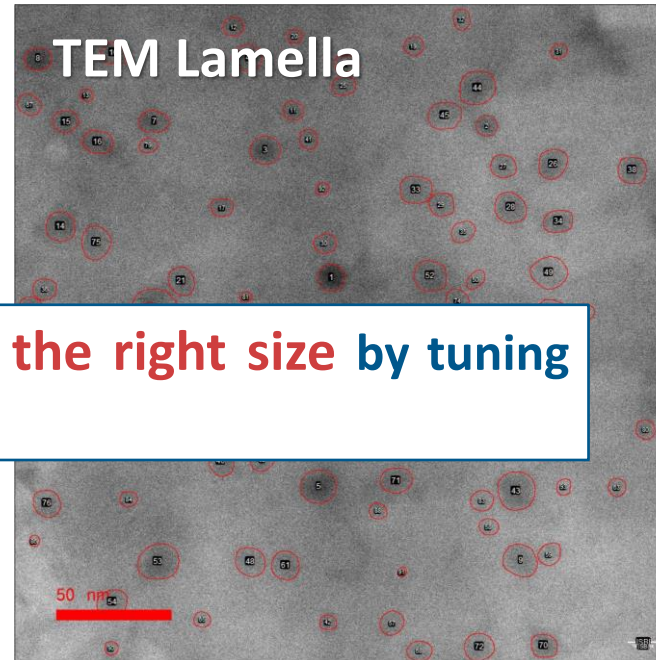
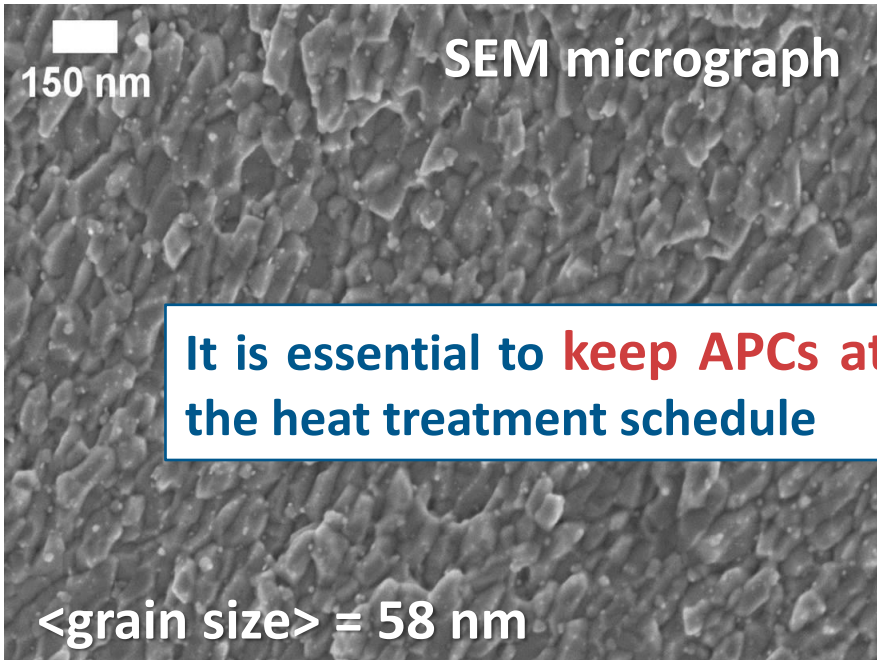
Internal Oxidation – APC – Nb-Ta-Hf alloy
non-Cu J_c calculated for a HL-LHC wire layout from the measured layer J_c . – non-Cu $J_c = 0.6$ layer J_c . Data from:

Bovone *et al.*, Supercond. Sci. Tech. **36** (2023) 095018
DOI: [10.1088/1361-6668/aced25](https://doi.org/10.1088/1361-6668/aced25)



Internal Oxidation at the nanoscale

- Starting alloy: Nb-Ta-Hf or Nb-Ta-Zr
- Oxygen supply: SnO₂ powders



The observed **enhancement of layer J_c** is robust and reproducible

Grain refinement and formation of nano-ZrO₂ (HfO₂) due to the oxidation of Zr (Hf)

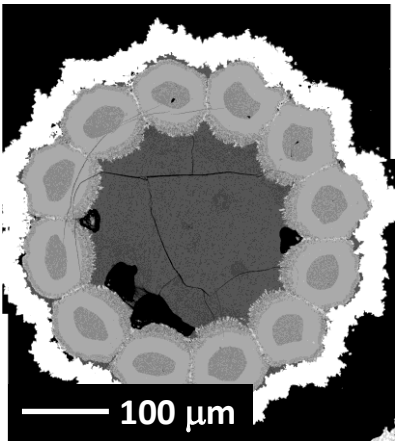
Nanoparticles are active as APCs only if their size is 3-4 nm comparable to $\xi(4.2 \text{ K})$ of Nb₃Sn

Internal Oxidation at the microscale

What needs to be done

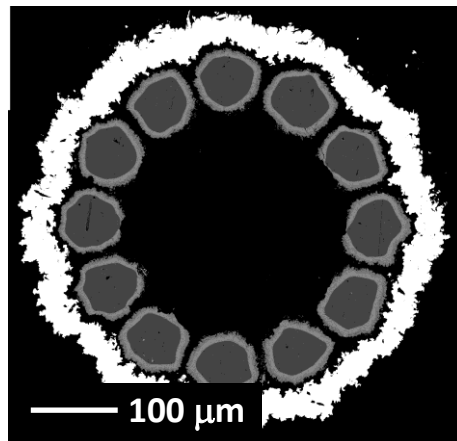
Simplified subelement after HT: 550°C x 100h + 650°C x 200h

Starting alloy: Nb-Ta-Hf



without oxygen source

Reaction layer = 20 μm



with oxygen source

Reaction layer = 4 μm

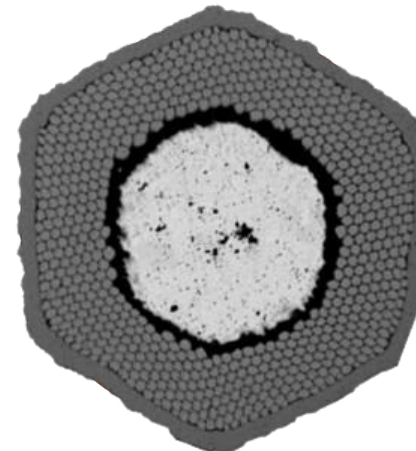
Reaction kinetics is slower

Optimization is needed for the composition of the application-ready subelement

Subelement composition to maximize non-Cu J_c

TABLE 1

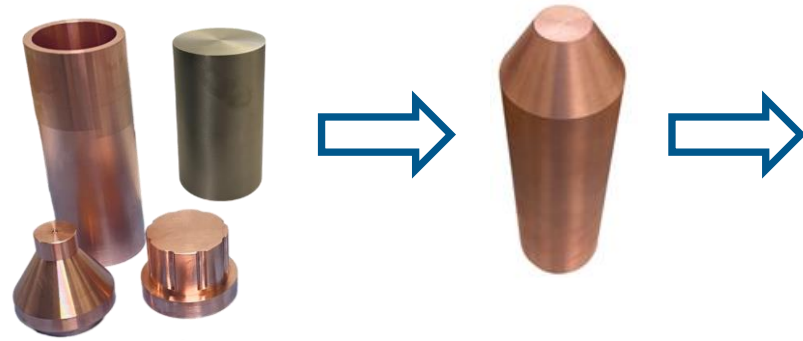
Parameter	Range	Preferred Range
Total Nb content	50-65% of Non-Cu	55-60% of Non-Cu
Sn wt % / ((Sn wt % + Cu wt %) within the diffusion barrier	45-65%	50-60%
Local Area Ratio	0.10-0.30	0.15-0.25
Nb to Sn atomic ratio	2.7-3.7	3.1-3.6
Nb filament diameter	0.5-7 microns	1-5 microns
Nb diff. barrier thickness	0.8-11 microns	1.5-8 microns
Nb barrier fraction of Nb	20-50%	25-35%



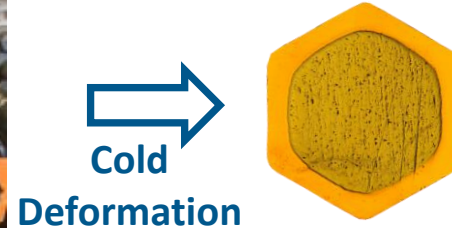
M. Field, J. Parrell, Y. Zhang, Patent US 7,368,021 B2

Internal Oxidation implemented in Wire Technology

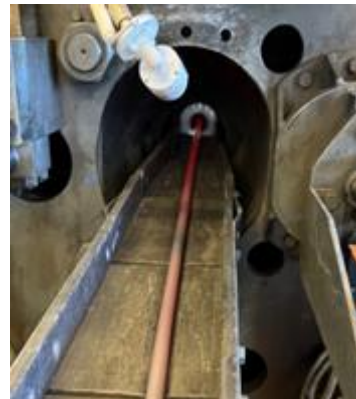
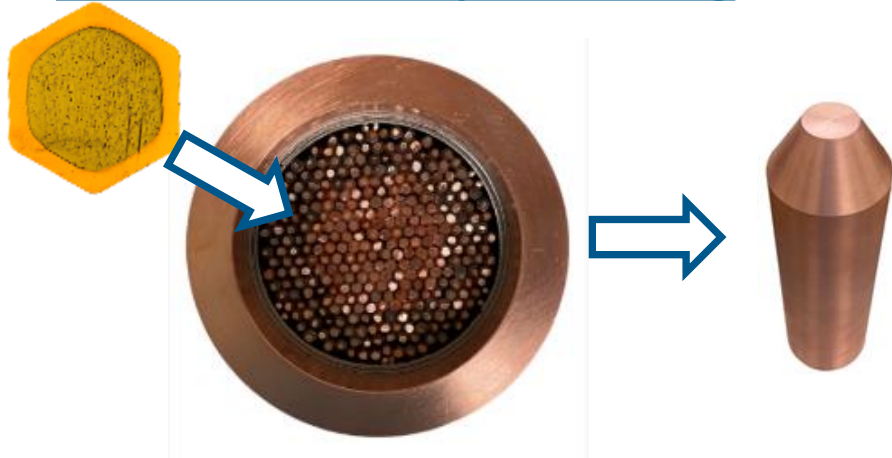
1. Filament processing



Hot Extrusion
(500°C – 600°C)

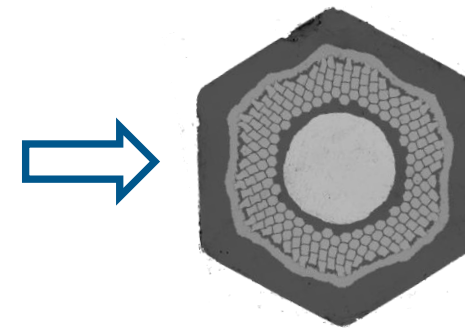


2. Subelement processing

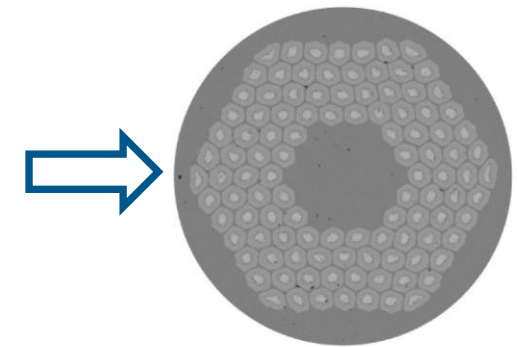


Hot Extrusion
(500°C – 600°C)

3. Wire processing



**Drilling,
Sn rod insertion
and cold deformation**



**Subelement restack
and cold deformation
to final diameter**

Hot Extrusion → Area Reduction ≈ 90%
Cold Deformation → Area Reduction ≈ 10%

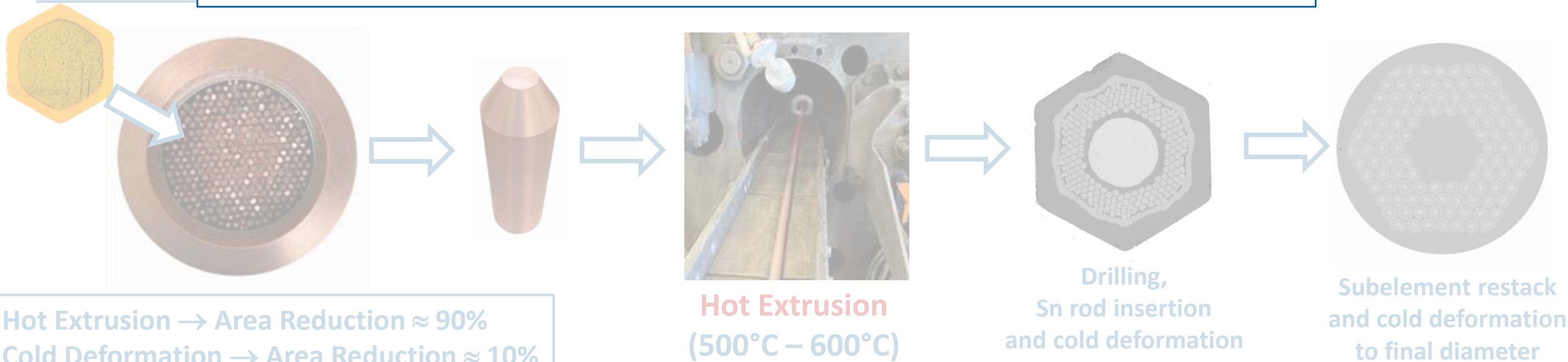
Internal Oxidation implemented in Wire Technology

1. Filament processing



It is essential to **impede the decomposition of the oxygen-rich powder** during the Hot Extrusion steps

2. Subelement



Hot Extrusion → Area Reduction \approx 90%
Cold Deformation → Area Reduction \approx 10%

Hot Extrusion
(500°C – 600°C)

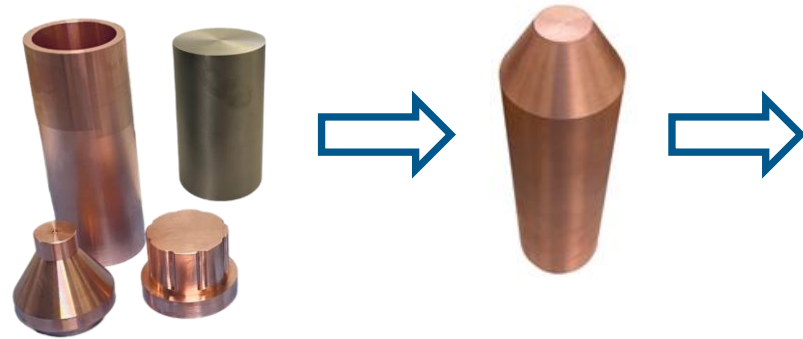
Drilling,
Sn rod insertion
and cold deformation

Subelement restack
and cold deformation
to final diameter

Internal Oxidation implemented in Wire Technology

Two strategies for including an oxygen supply in the wire composite

1. Filament processing



Hot Extrusion
(500°C – 600°C)

Cold
Deformation

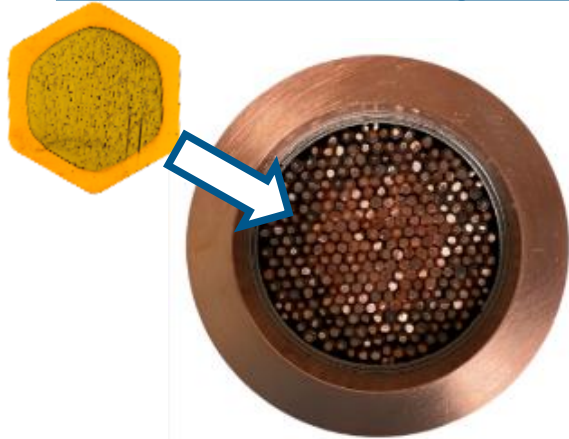


Strategy #1:

At the filament level

Pro: Fine distribution of the oxygen supply
Con: Oxygen-rich powders must withstand two Hot Extrusions

2. Subelement processing



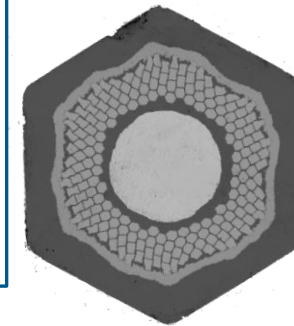
Strategy #2:

At the subelement level

Pro: Oxygen-rich powders must withstand only one Hot Extrusion
Con: Coarser distribution of the oxygen supply



Hot Extrusion
(500°C – 600°C)

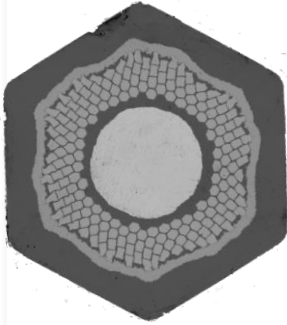


Drilling,
Sn rod insertion
and cold deformation

Hot Extrusion → Area Reduction ≈ 90%
Cold Deformation → Area Reduction ≈ 10%

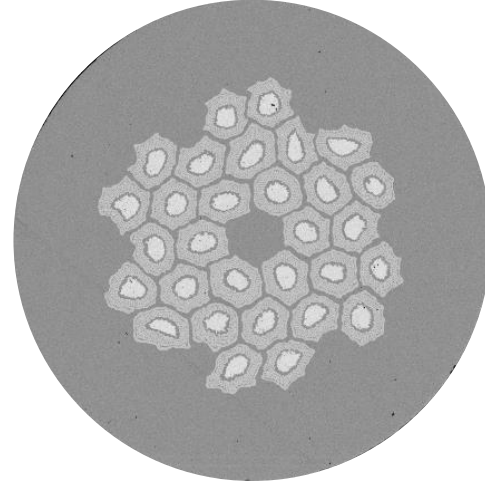
Wire portfolio: developing the fabrication process

Reference wires without Internal Oxidation

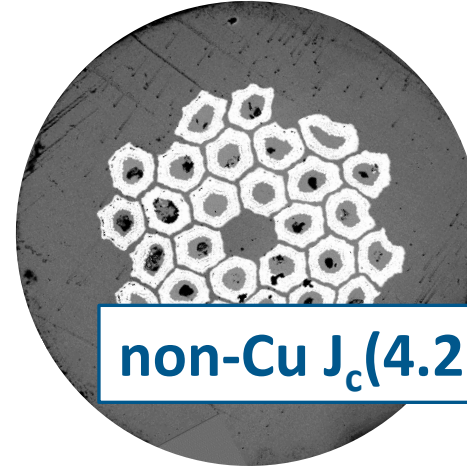


$\varnothing = 1.16$ mm

Subelement assembly
192 Cu/Nb-Ta filaments

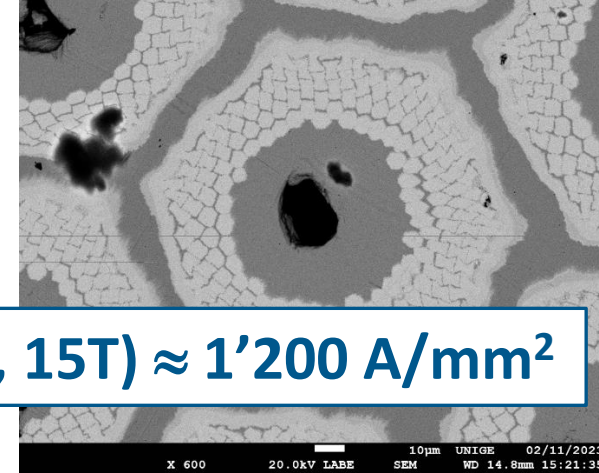


30/37 restack, $\varnothing = 1.12$ mm
before heat treatment

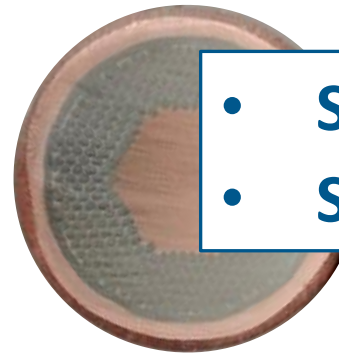
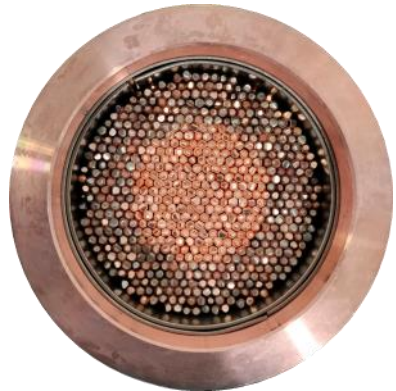


30/37 restack, $\varnothing = 1.12$ mm
after heat treatment

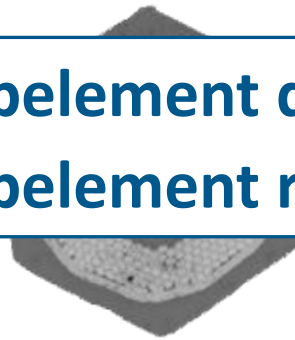
non-Cu $J_c(4.2K, 15T) \approx 1'200$ A/mm²



Reacted subelement



$\varnothing = 18$ mm

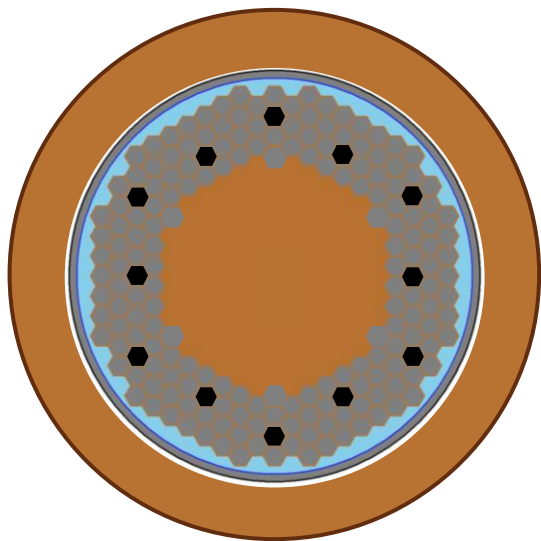


$\varnothing = 1.16$ mm

Subelement assembly
390 Cu/Nb-Ta filaments

- Subelement deformation with Nb-Ta alloy is successful
- Subelement restacking into long wire remains challenging

Internal Oxidation implemented at the subelement level



Subelement assembly
180 Cu/Nb-alloy filaments
12 Cu tubes containing SnO₂
(oxygen supply)

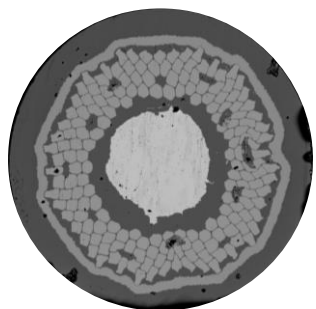


Subelement assembly
Ø 70 mm

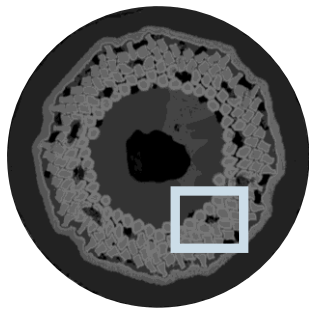


Hot extruded rod
Ø 18 mm

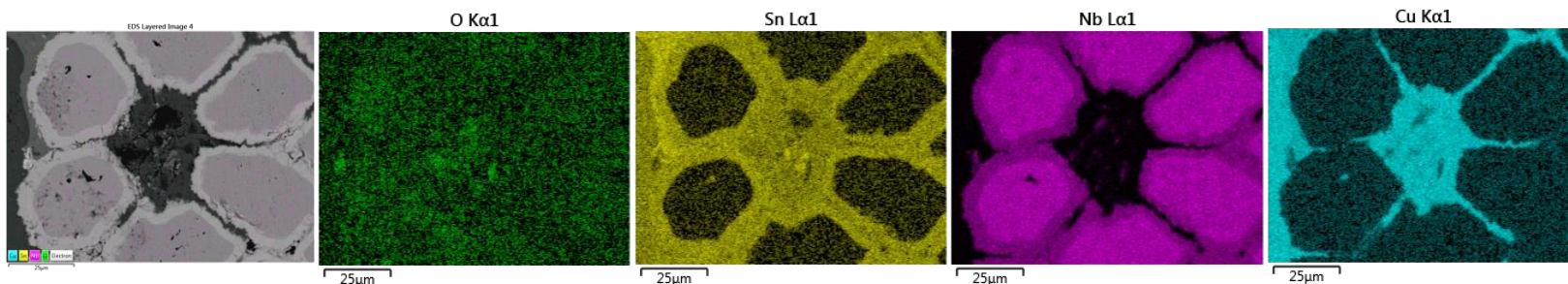
Good news #1
No decomposition of SnO₂
after Hot Extrusion



Drawn to Ø 1.0 mm
before heat treatment

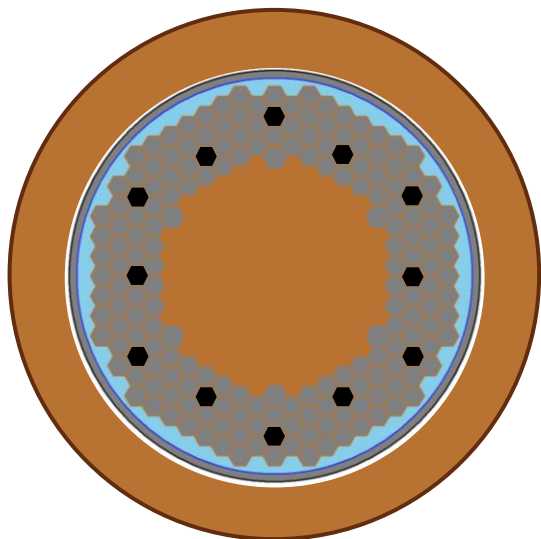


Drawn to Ø 1.0 mm
after heat treatment
210°C/50h + 400°C/50h +
650°C/200 h



Good news #2
Decomposition of SnO₂ after reaction
heat treatment

Internal Oxidation implemented at the subelement level



Subelement assembly

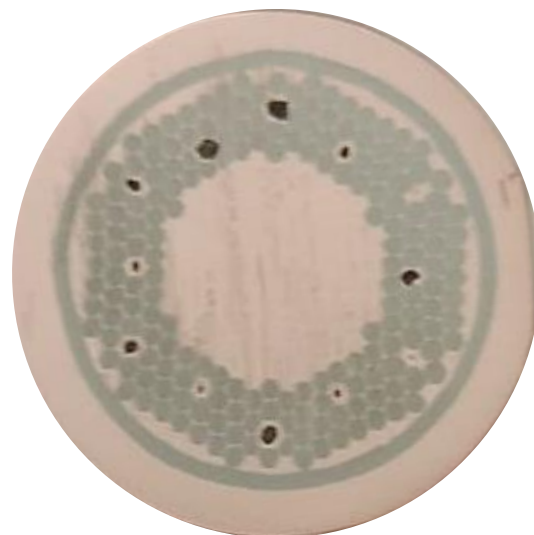
180 Cu/Nb-alloy filaments

12 Cu tubes containing SnO_2
(oxygen supply)



Subelement assembly

Ø 70 mm



Hot extruded rod

Ø 18 mm



Not only good news...

- longitudinal "sausaging" and accumulation of the SnO_2 powders observed after Hot Extrusion
- Difficulties in extruding subelements made from ternary alloys (Nb-Ta-Hf and Nb-Ta-Zr), due to higher work hardening compared with Nb-Ta

Wire technology: Wrap Up

Completed

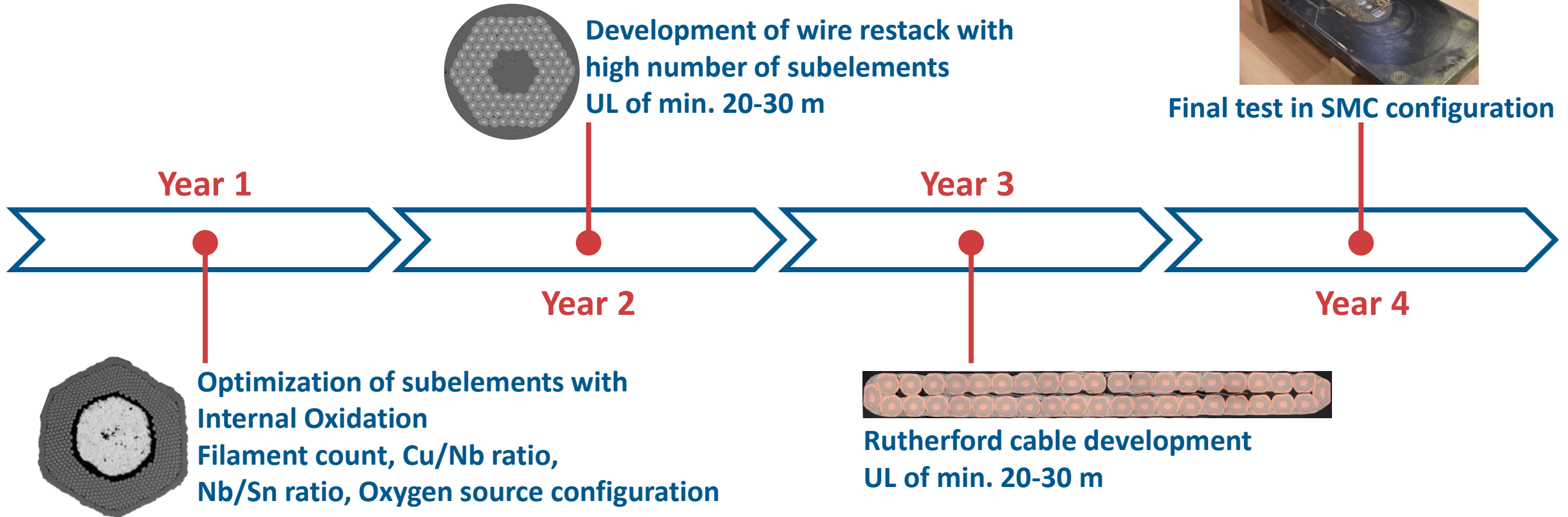
- **22 extrusion billets produced to date: 7 filaments and 15 subelements**
- **Consolidated process for producing RRP-like subelements, currently available only in a limited number of industrial facilities worldwide**
- **Two strategies identified for implementing Internal Oxidation within the subelement**
- **Methods developed to preserve the oxygen-rich powder from decomposition during hot extrusion**
- **Ongoing development of solutions enabling hot extrusion of subelements based on ternary alloys (Nb–Ta–Hf and Nb–Ta–Zr)**

To be done

- **Optimization of subelement composition to account for slower reaction kinetics in the presence of internal oxidation**
- **Development of methods to mitigate longitudinal “sausaging” of the oxygen source after hot extrusion**
- **Development of processes for producing long-length wires with a high subelement count**

What should be next

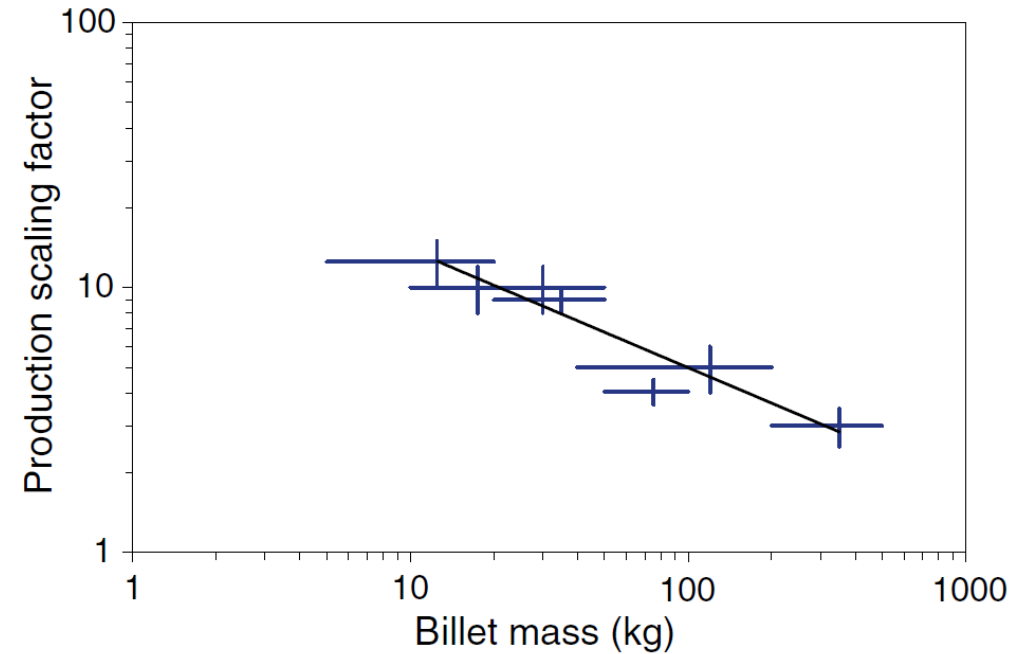
Towards industrialization



Cost and Price estimates

after Cooley *et al.*, *Supercond. Sci. Tech.* **18** (2005) R51
DOI: [10.1088/0953-2048/18/4/R01](https://doi.org/10.1088/0953-2048/18/4/R01)

Strand type	Internal Sn HEP			
	c. 2003	Var. 1	Var. 2	
(A) Materials and geometry				
Superconductor	Nb7.5Ta	Nb	Nb + Nb47Ti	Nb7.5Ta2Hf
Stabilizer	Cu	Cu	Cu	Cu
Reactants	Sn	Sn3Ti	Sn	Sn
Diffusion barrier	Nb	Nb	Nb	Nb
Ancillary materials ^a	Cu	Cu	Cu	Cu
Reactants area fraction (%)	13	13	13	13
Diffusion barrier area fraction (%)	8	8	8	8
Ancillary materials area fraction (%)	4	4	4	4
Superconductor area fraction ^b (%)	25 ^d	25 ^d	25 ^d	23.5
Oxygen supply area fraction (%)				1.5
(B) Performance				
<u>Non-stabilizer J_c (A mm⁻²)</u>				
10 T	4850	4850	4850	4950
12 T	3000	3000	3000	3700
15 T	1600	1600	1600	2250
20 T	400	400	400	580
(C) Raw materials costs				
			(2026)	
Superconductor cost (\$ kg ⁻¹)	290	220	200	400
Stabilizer cost (\$ kg ⁻¹)	5	5	5	15
Reactants cost (\$ kg ⁻¹)	15	110	15	15
Diffusion barrier cost (\$ kg ⁻¹)	220	220	220	400
Ancillary materials cost (\$ kg ⁻¹)	5	5	5	15
Oxygen supply (\$ kg ⁻¹)				60
(D) Cost indices				
Raw materials (\$ kg ⁻¹)	96	90	73	142
Raw materials (\$ m ⁻¹)	0.43	0.40	0.32	0.62
relative to LHC strand	2.4	2.2	1.7	
Raw materials (\$ kA ⁻¹ m ⁻¹)				
10 T	0.35	0.32	0.26	
12 T	0.56	0.52	0.42	
15 T	1.00	0.97	0.78	1.5 \$/kAm
20 T	4.20	3.90	3.13	1.25 \$/kAm
Purchase price @ 1:1, 0.8 mm	1000 \$ kg ⁻¹			1500 \$kg ⁻¹
Production scaling factor P	10.4	(10.4)	(10.4)	(10.4)
$P/P(\text{LHC})$	3.2			
Scaled strand (\$ m ⁻¹)	4.36	4.06	3.27	
Scaled cable (\$ m ⁻¹) ^c	166	154	125	
Scaled strand (\$ kA ⁻¹ m ⁻¹)				
10 T	3.60	3.40	2.72	
12 T	5.80	5.40	4.34	
15 T	11	10	8.20	16 \$/kAm
20 T	44	40	33	13 \$/kAm



$$\text{Production Scaling Factor } P = \frac{\text{Purchase Price}}{\text{Raw Material Cost}}$$

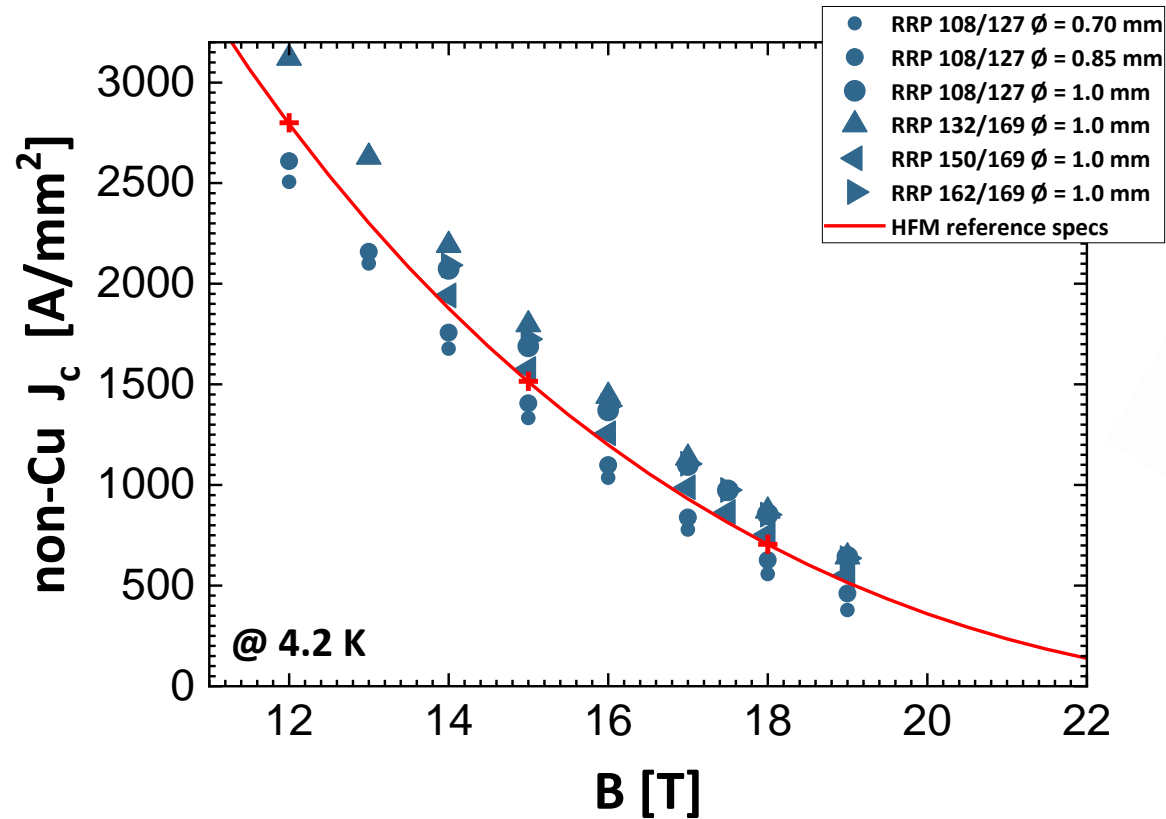
An estimated price reduction by ~20% with Internal Oxidation and APCs

Outline

- Towards application-ready Nb₃Sn wires with enhanced performance
 - **Internal Oxidation** and **APCs**: material properties and practical implementation
- **Electromechanical properties of state-of-the-art Nb₃Sn wires**
 - Effects of the **longitudinal strain** on magnet design **margins**
 - Influence of the **wire layout** on the **transverse stress tolerance**
- Summary and conclusions

Performance of state-of-the-art wires

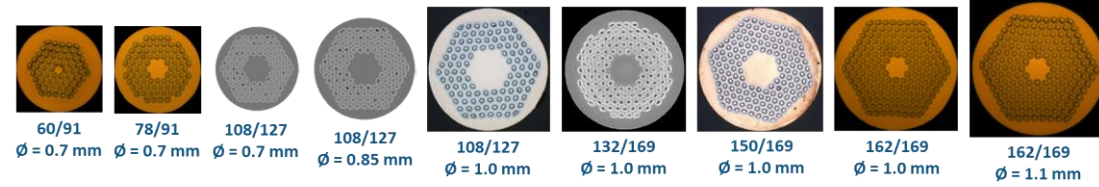
HL-LHC & HFM RRP wires and HFM specs



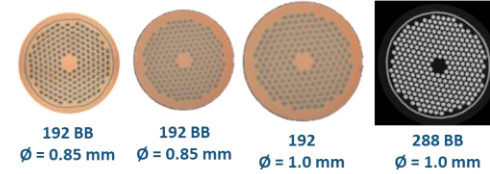
R. Babouche, HFM Forum (2025)

URL: indico.cern.ch/event/1543973/

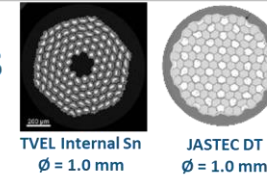
RRP



PIT



Others

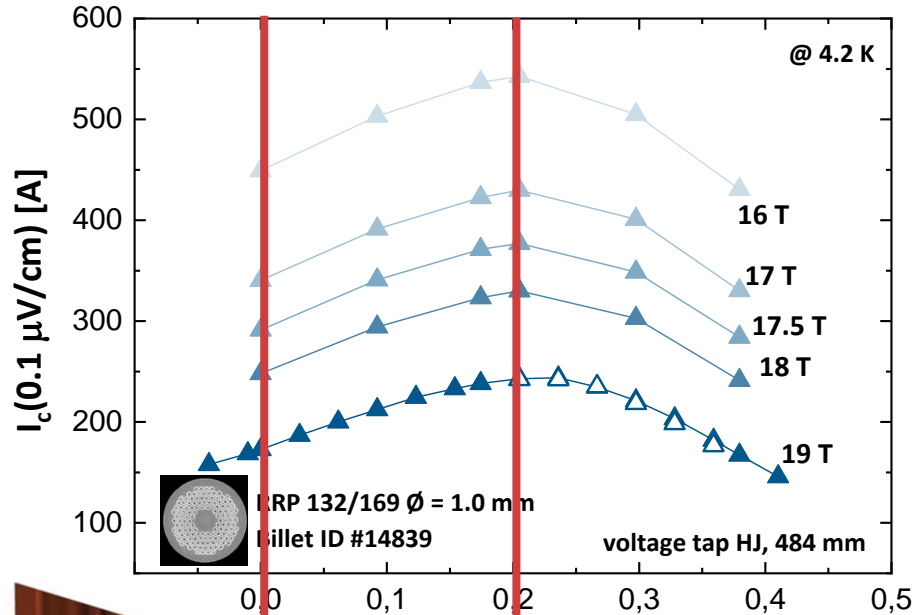


Ti barrel

- I_c measurements are performed on a Ti barrel
- Nb_3Sn is under longitudinal precompression after free-standing cooldown
- The Ti barrel imposes a longitudinal tension on the wire
- The resulting strain-state of the wire is undetermined

What has been tested beyond I_c

Critical current vs longitudinal strain and transverse stress



Applied longitudinal strain [%]

Zero applied strain, $\epsilon = 0\%$

Wire with its precompression

Maximum of I_c , $\epsilon = \epsilon_{\text{max}}$

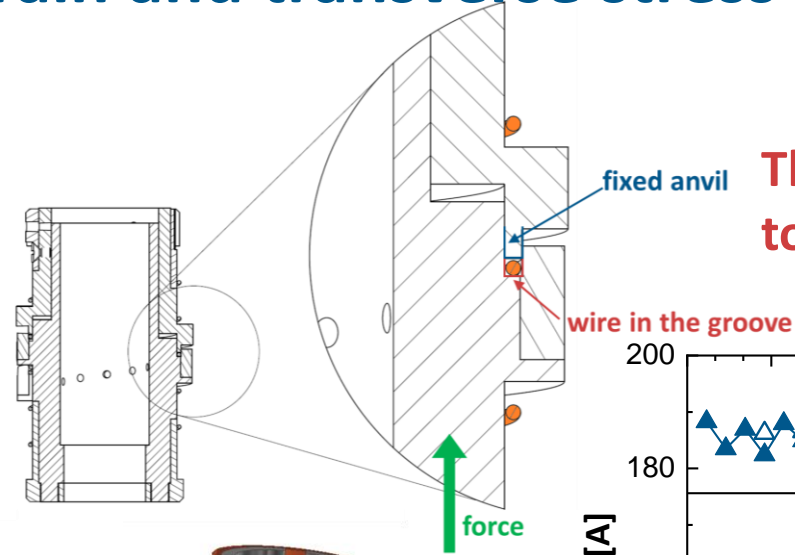
Precompression released

Walters *et al.*, *Cryogenics* **26** (1986) 406

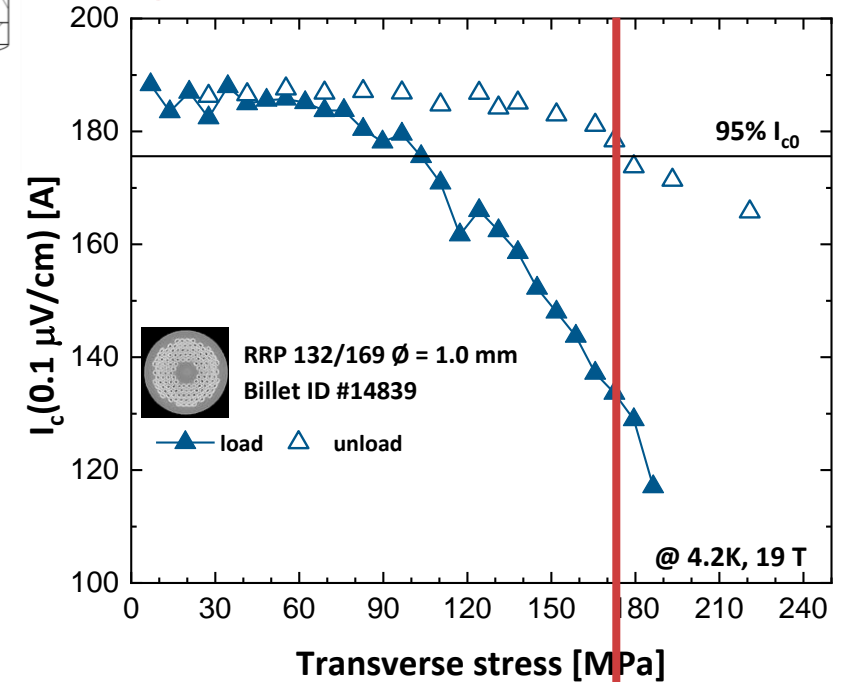
DOI: [10.1016/0011-2275\(86\)90085-8](https://doi.org/10.1016/0011-2275(86)90085-8)

Seeber *et al.*, *Rev. Sci. Instrum.* **76** (2005) 093901

DOI: [10.1063/1.2018608](https://doi.org/10.1063/1.2018608)

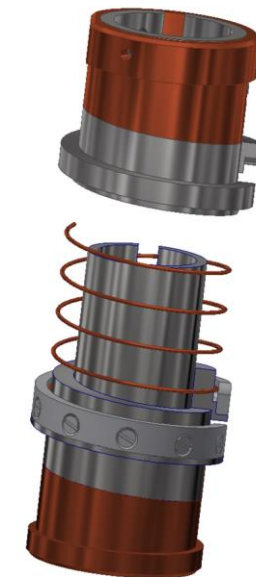


The WASP concept adapted to transverse loads



Irreversible limit

$\sigma_{\text{irr}} (B=19\text{T}) = 172$ MPa

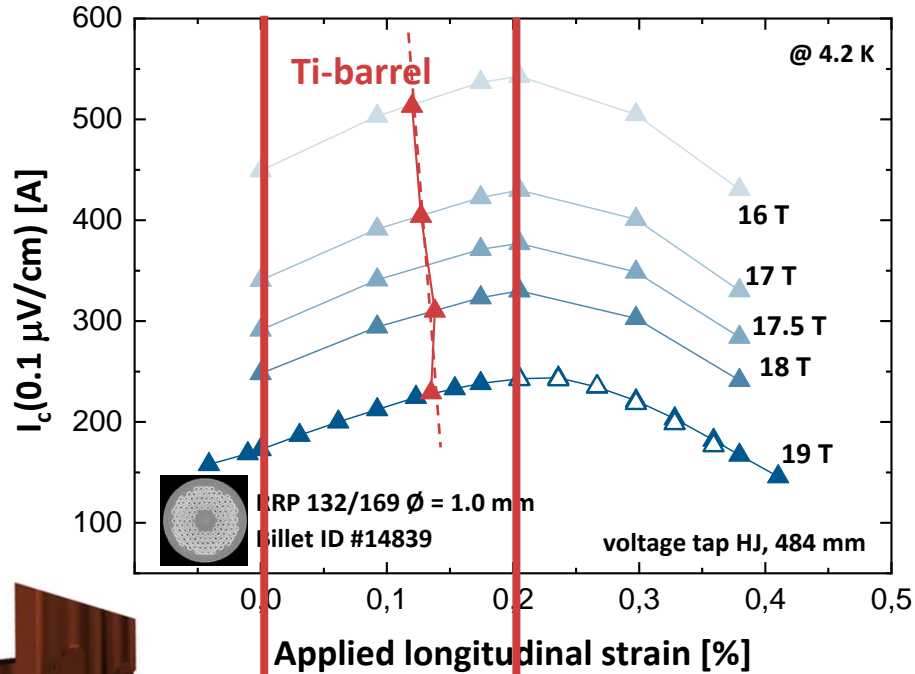


Seeber *et al.*, *IEEE TAS* **17** (2007) 2643

DOI: [10.1109/TASC.2007.897934](https://doi.org/10.1109/TASC.2007.897934)

What has been tested – Electromechanical properties

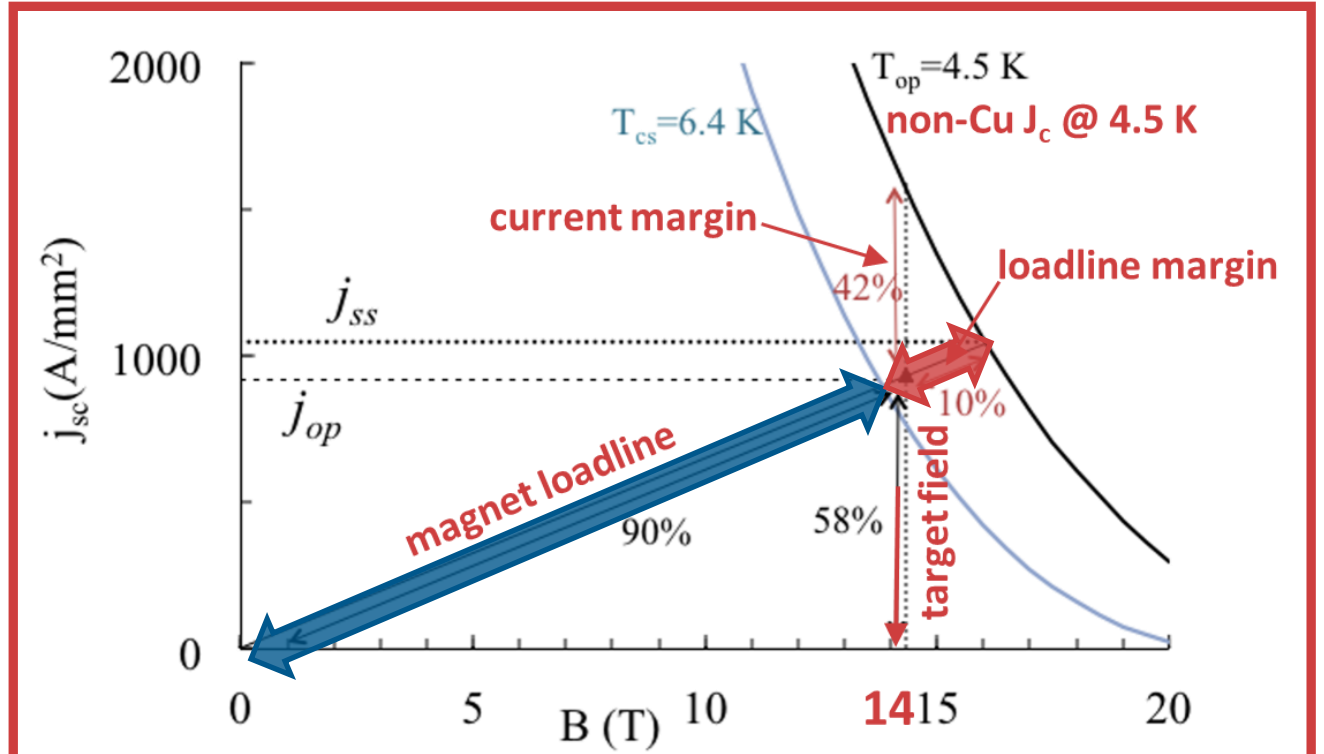
Critical current vs longitudinal strain and transverse stress



Zero applied strain, $\varepsilon = 0\%$

Wire with its precompression

Maximum of I_c , $\varepsilon = \varepsilon_{\text{max}}$
Precompression released



How strong is the influence of strain on margins?

Walters *et al.*, *Cryogenics* **26** (1986) 406

DOI: [10.1016/0011-2275\(86\)90085-8](https://doi.org/10.1016/0011-2275(86)90085-8)

Seeber *et al.*, *Rev. Sci. Instrum.* **76** (2005) 093901

DOI: [10.1063/1.2018608](https://doi.org/10.1063/1.2018608)

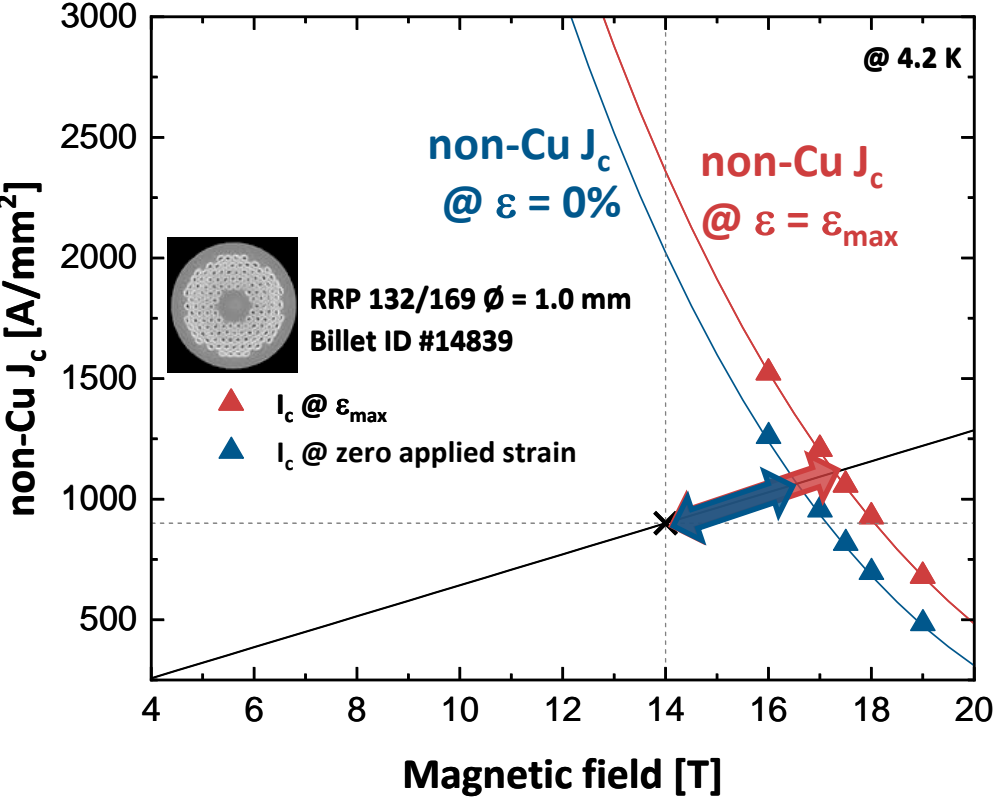
Todesco, HFM Forum (2025), URL: indico.cern.ch/event/1544424/

FCC Feasibility Study Report and ESPPU documents

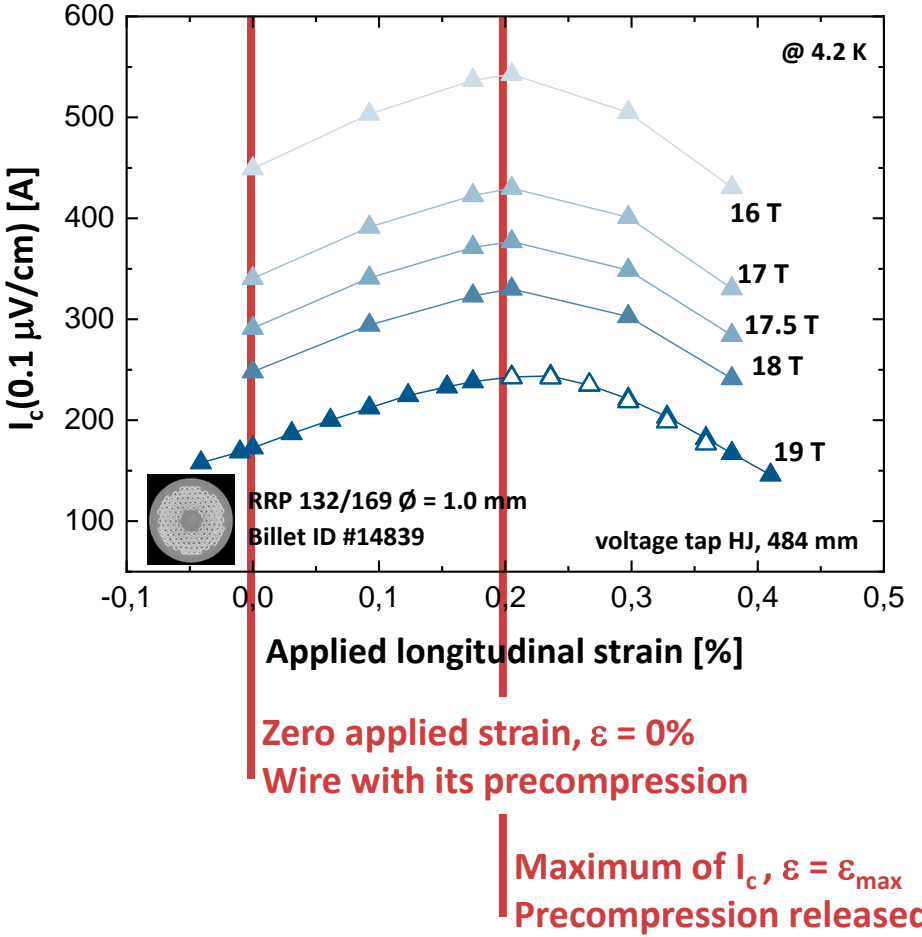
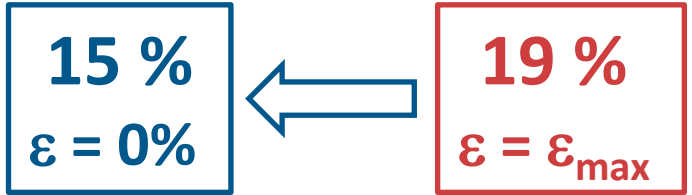
<https://indico.cern.ch/event/1534205/>

Loadline margin vs longitudinal strain

RRP 132/169, $\phi = 1.0$ mm



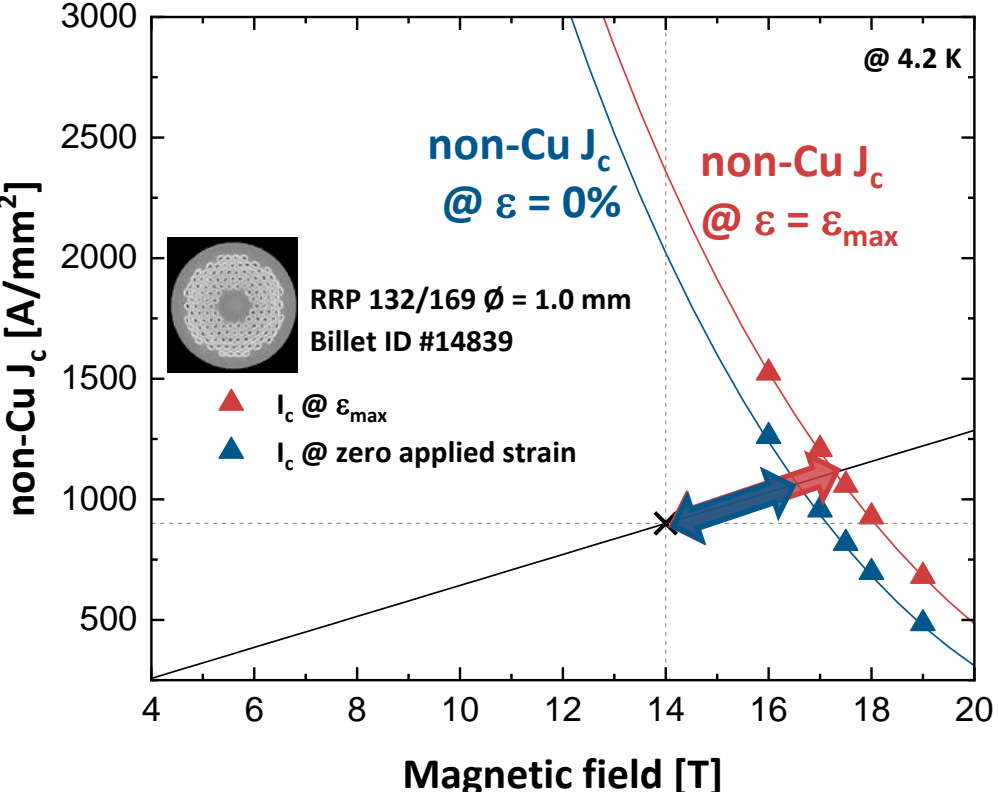
Loadline margin @ $T_{op} = 4.2$ K



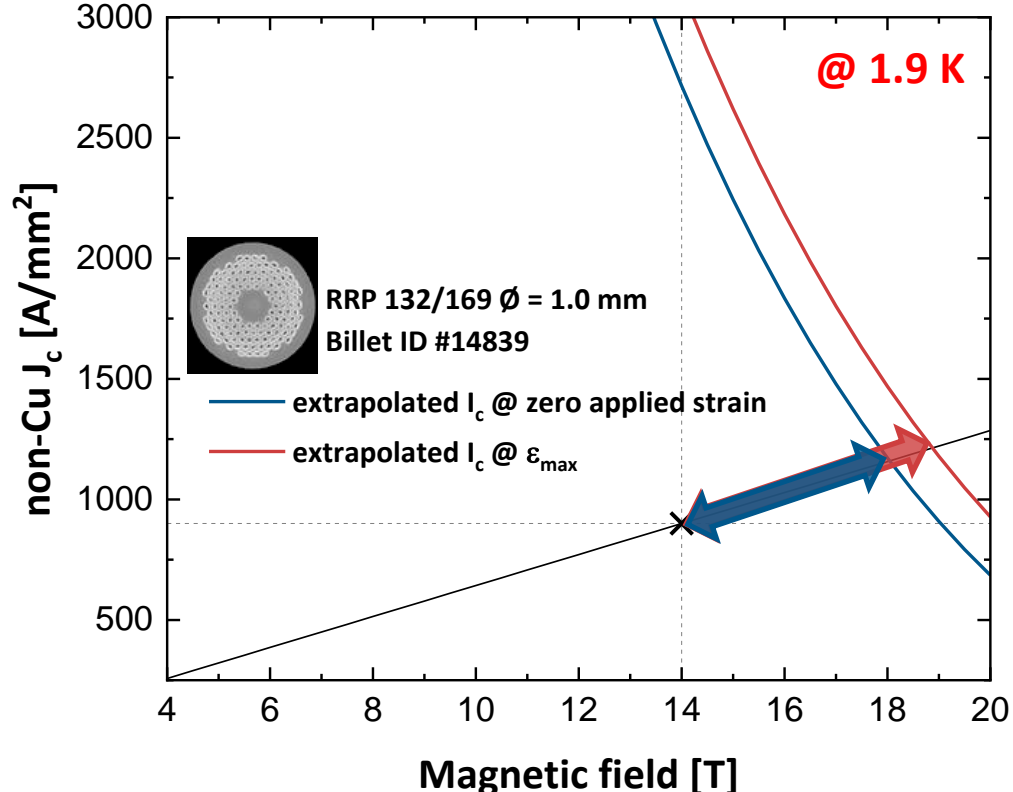
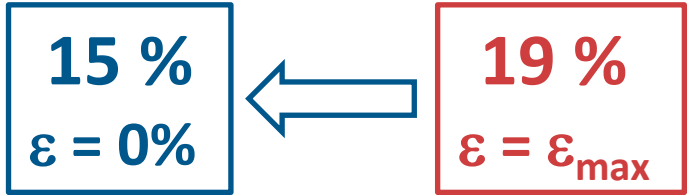
Maximum of I_c , $\epsilon = \epsilon_{max}$
Precompression released

Loadline margin vs longitudinal strain

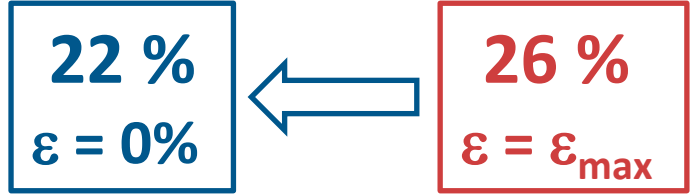
RRP 132/169, $\phi = 1.0$ mm



Loadline margin @ $T_{op}=4.2K$

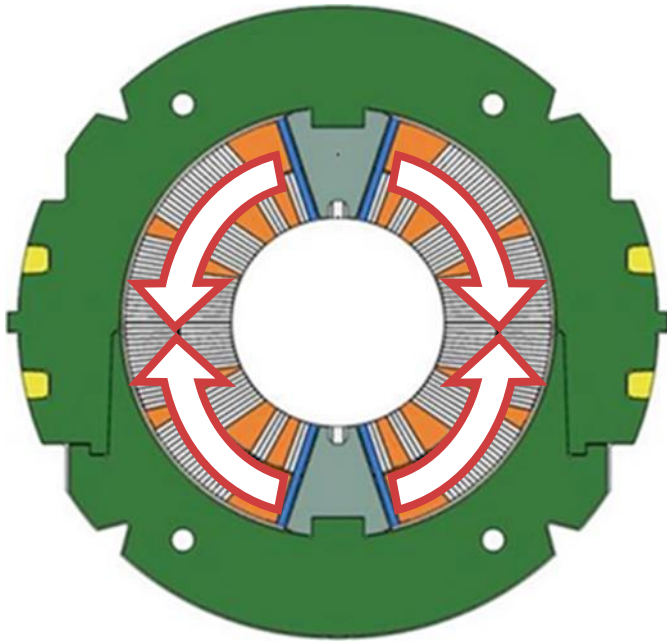


Calculated Loadline margin @ $T_{op}=1.9K$



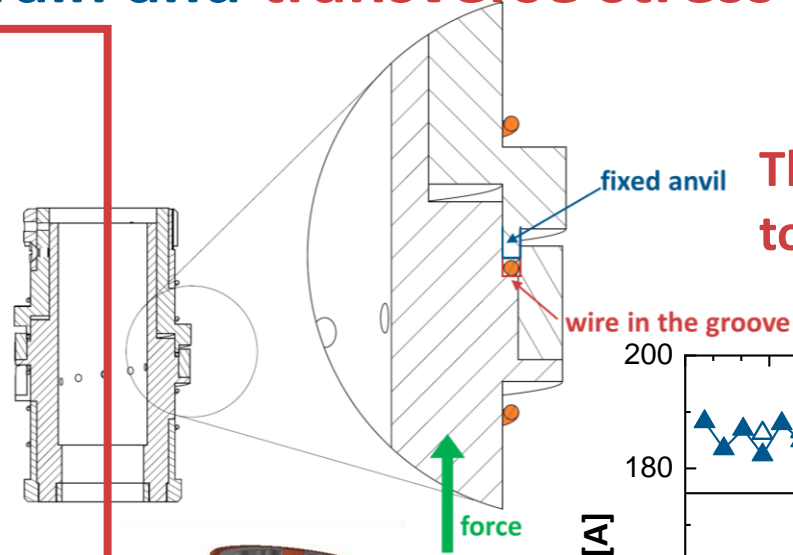
What has been tested – Electromechanical properties

Critical current vs longitudinal strain and transverse stress

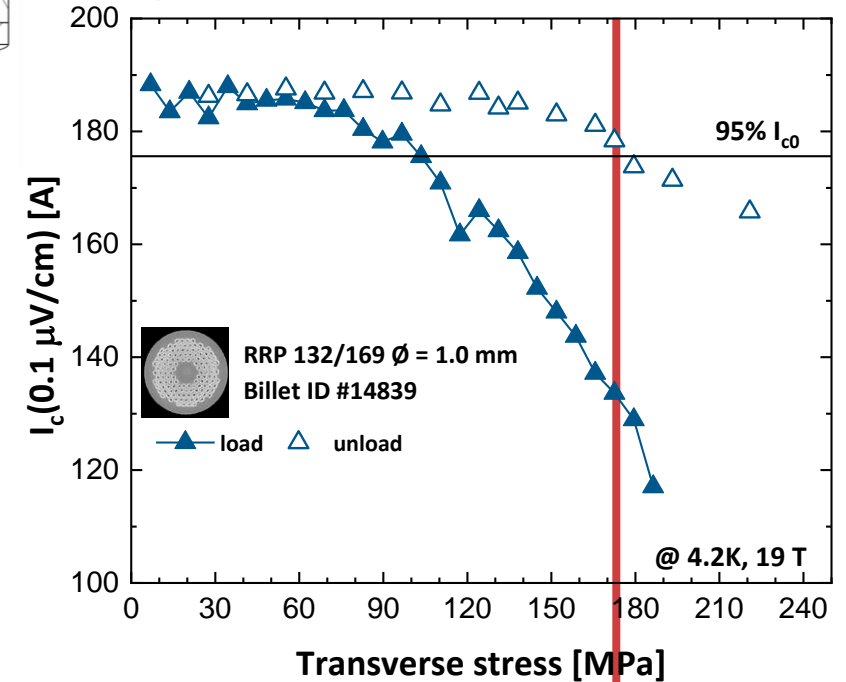
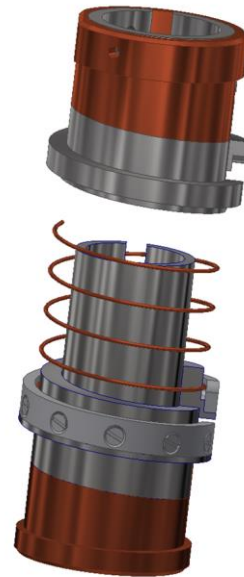


A combination of electromagnetic forces with pre-load and thermomechanical effects exposes the brittle and strain sensitive Nb_3Sn to the risk of degradation

Even if the peak stress when the magnet is energized is at the midplane, large stresses at the pole after pre-load and cooldown can induce permanent reduction of I_c



The WASP concept adapted to transverse loads

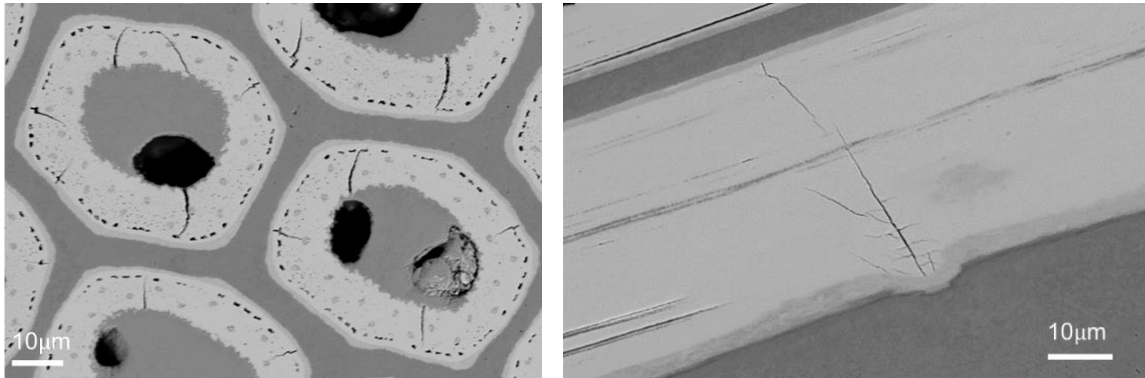


Irreversible limit
 σ_{irr} (B=19T) = 172 MPa

Irreversible reduction of the critical current after unload

Two mechanisms govern the permanent reduction of the critical current under transverse stress

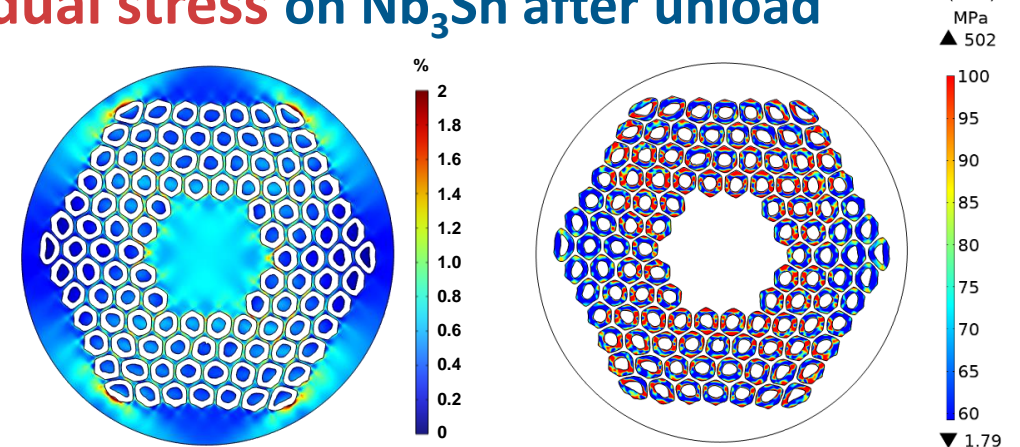
Formation of **cracks** in the Nb₃Sn filaments



Lenoir *et al.*, Supercond. Sci. Technol. **37** (2024) 025013
DOI: [10.1088/1361-6668/ad1341](https://doi.org/10.1088/1361-6668/ad1341)

Cracks generate a reduction of the current carrying cross section

Plastic deformation of the Cu matrix producing **residual stress** on Nb₃Sn after unload



Plastic strain in Cu after unload from 30 kN

von Mises stress in Nb₃Sn after unload from 30 kN (residual stress)

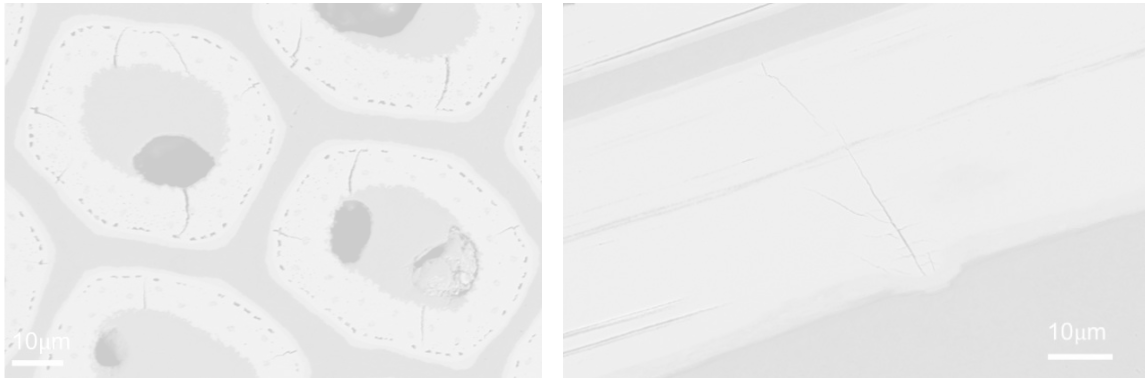
Bagni *et al.*, Supercond. Sci. Technol., **37** (2024) 095013
DOI: [10.1088/1361-6668/ad6a9c](https://doi.org/10.1088/1361-6668/ad6a9c)

Residual stress induces a permanent reduction of B_{c2}

Irreversible reduction of the critical current after unload

Two mechanisms govern the permanent reduction of the critical current under transverse stress

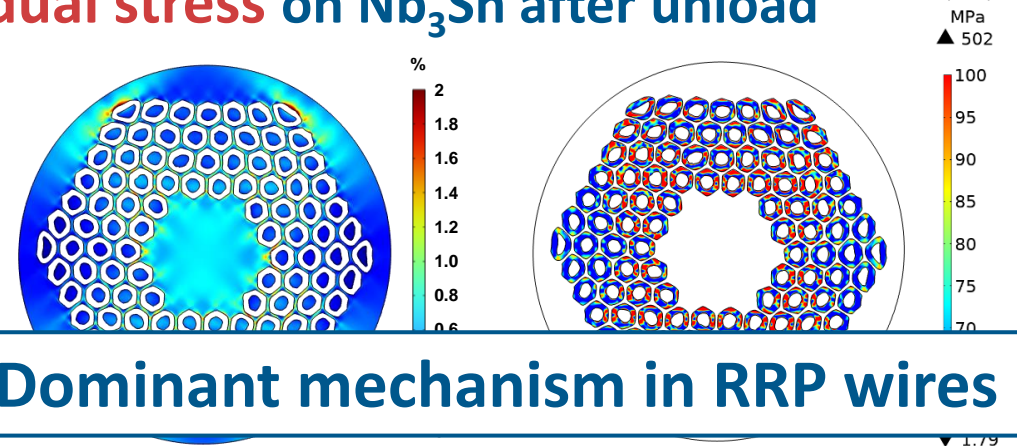
Formation of **cracks** in the Nb₃Sn filaments



Lenoir *et al.*, Supercond. Sci. Technol. **37** (2024) 025013
DOI: [10.1088/1361-6668/ad1341](https://doi.org/10.1088/1361-6668/ad1341)

Cracks generate a reduction of the current carrying cross section

Plastic deformation of the Cu matrix producing **residual stress** on Nb₃Sn after unload



Dominant mechanism in RRP wires

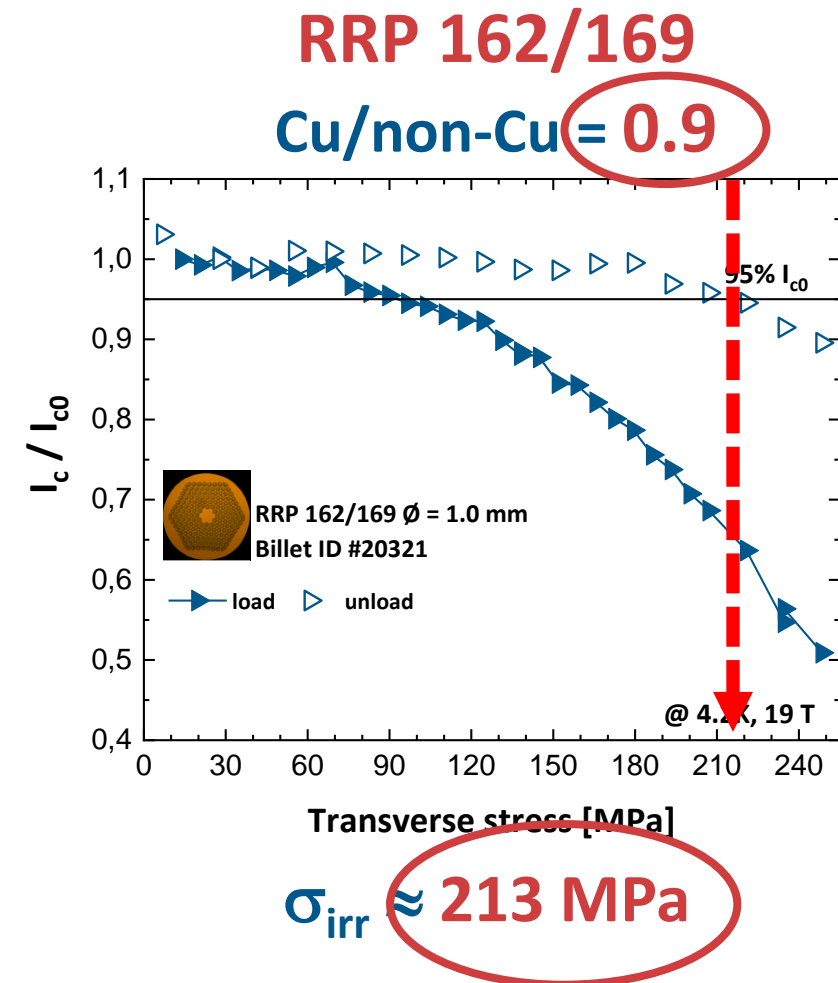
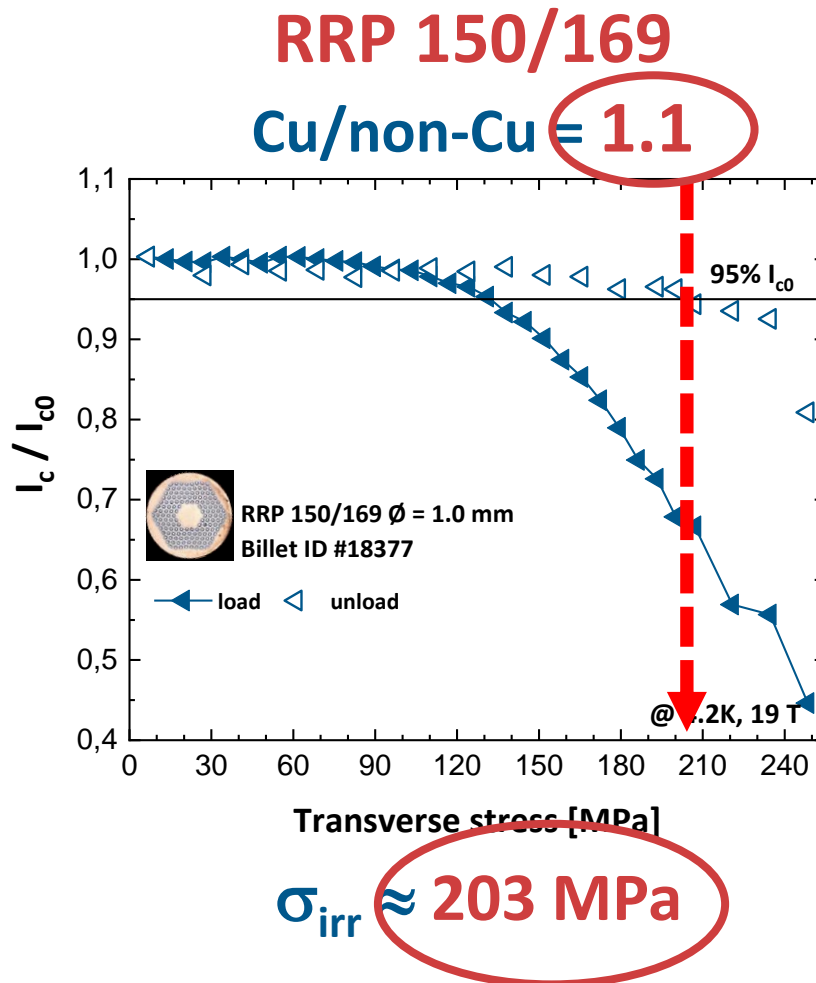
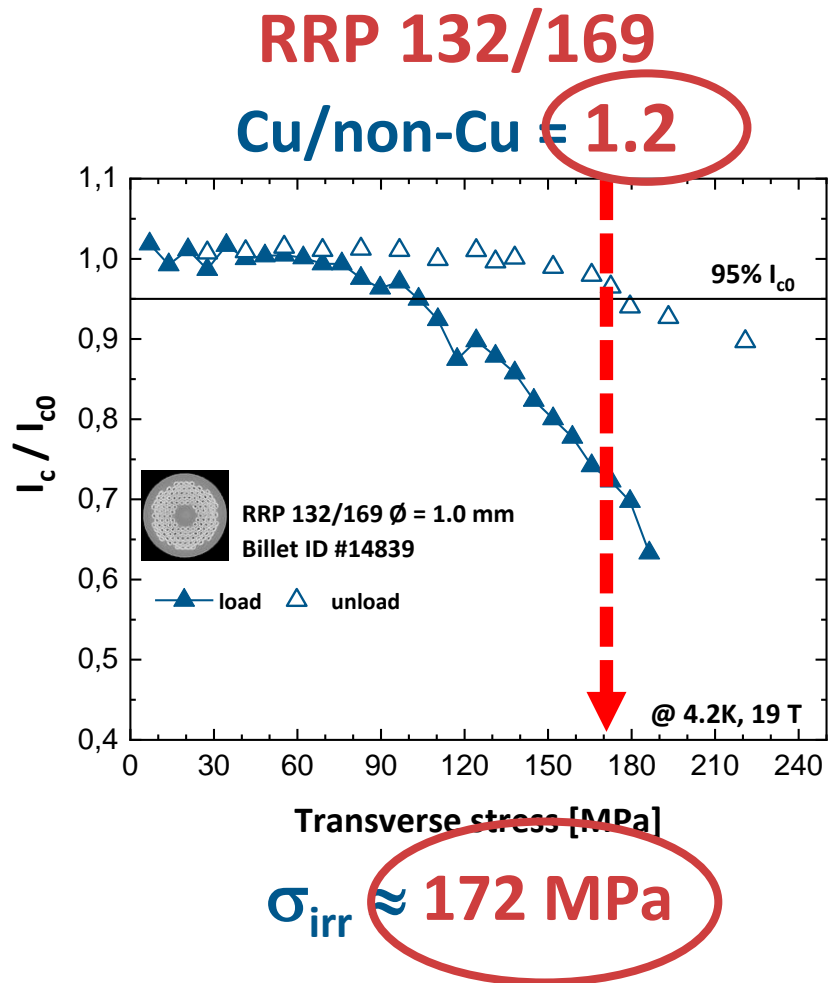
Plastic strain in Cu after unload from 30 kN

von Mises stress in Nb₃Sn after unload from 30 kN (residual stress)

Bagni *et al.*, Supercond. Sci. Technol., **37** (2024) 095013
DOI: [10.1088/1361-6668/ad6a9c](https://doi.org/10.1088/1361-6668/ad6a9c)

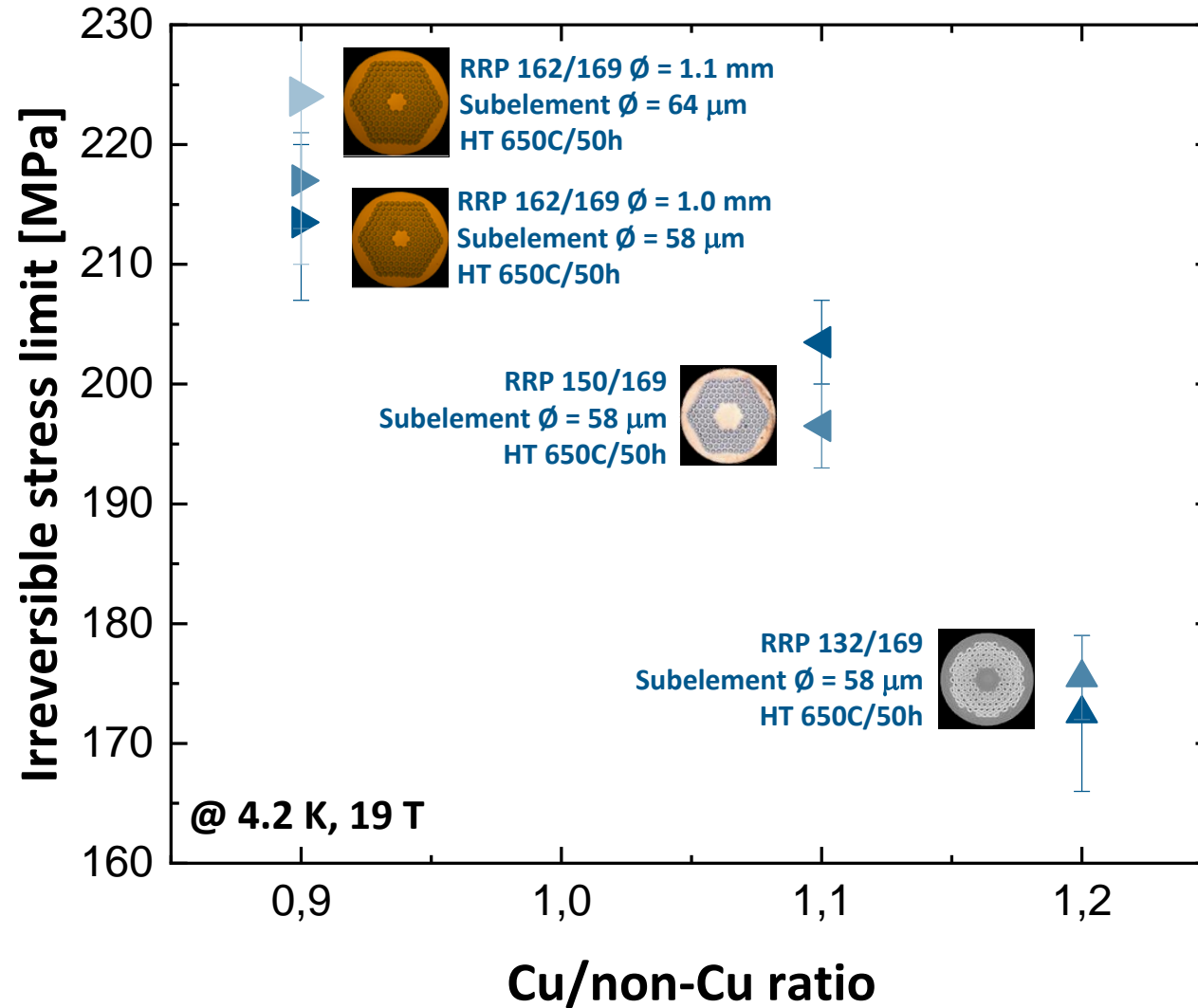
Residual stress induces a permanent reduction of B_{c2}

Irreversible stress limits at B = 19 T



A clear trend: the lower the Cu/non-Cu ratio, the higher the irreversible stress limit

Irreversible stress limits at B = 19 T

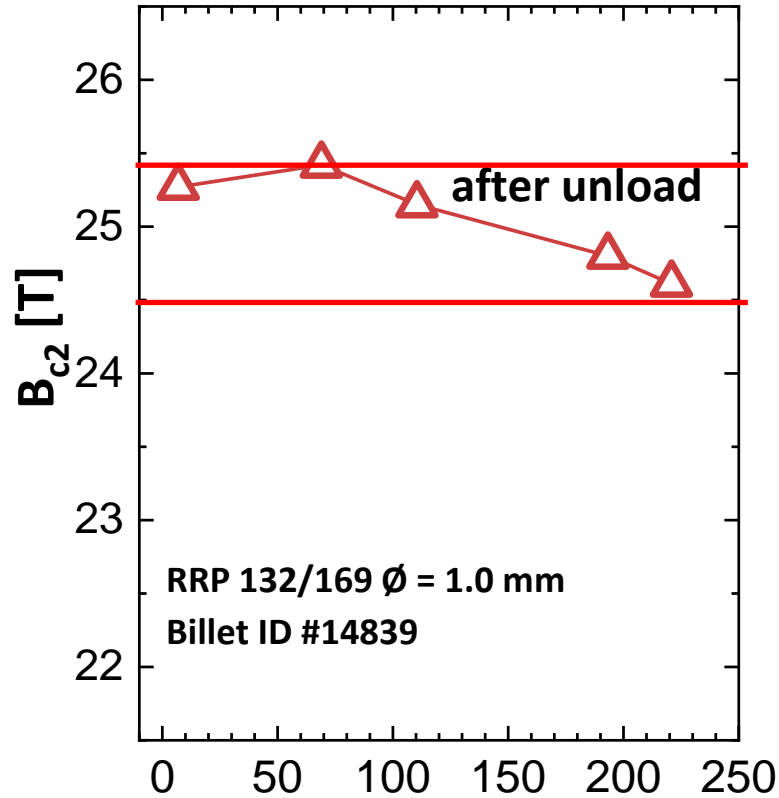


A clear trend: the lower the Cu/non-Cu ratio, the higher the irreversible stress limit

Comparison of B_{c2} after unload, different wire layouts

(as determined from Kramer extrapolation)

132/169, $\phi = 1.0$ mm

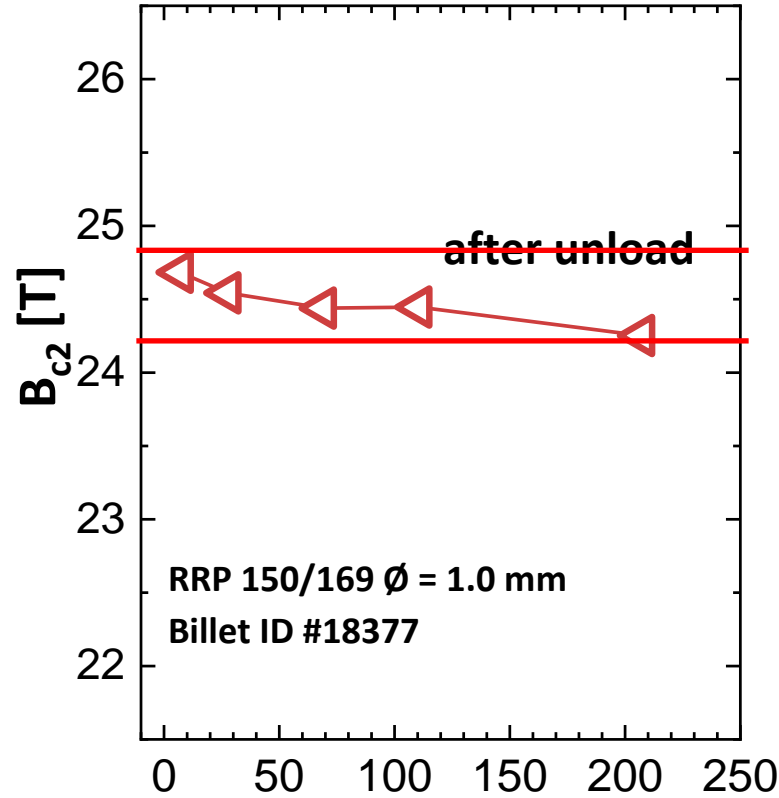


Transverse stress [MPa]

After unload from $\sigma = 210$ MPa

$$\Delta B_{c2}^{\text{unload}} \approx 1.0 \text{ T}$$

150/169, $\phi = 1.0$ mm

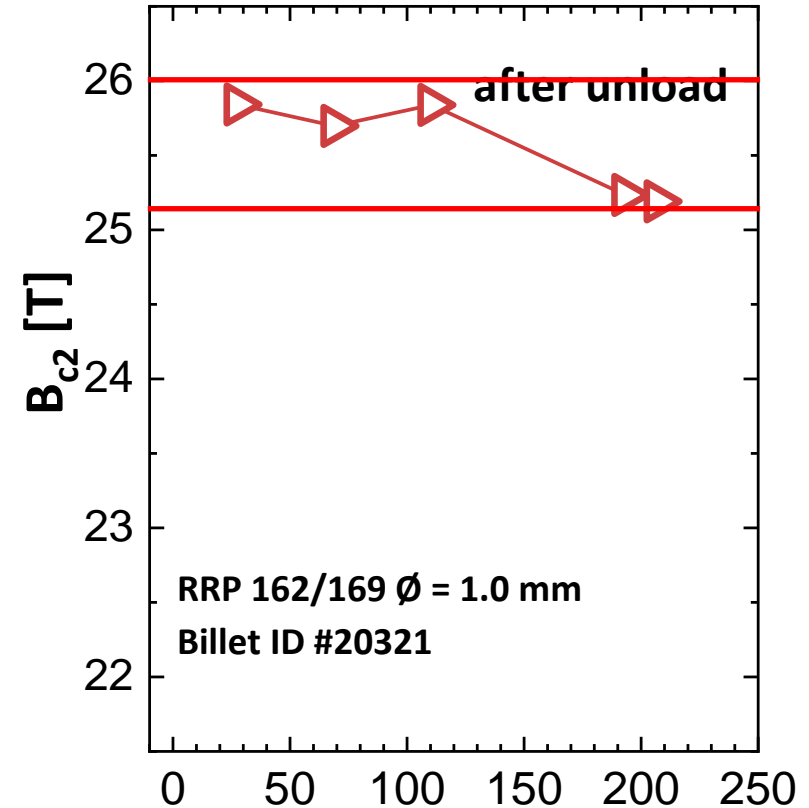


Transverse stress [MPa]

After unload from $\sigma = 210$ MPa

$$\Delta B_{c2}^{\text{unload}} \approx 0.4 \text{ T}$$

162/169, $\phi = 1.0$ mm



Transverse stress [MPa]

After unload from $\sigma = 210$ MPa

$$\Delta B_{c2}^{\text{unload}} \approx 0.65 \text{ T}$$

Summary and outlook

Advanced Wire Development

- Practical solutions to implement Internal Oxidation in RRP-like subelements are being developed at UNIGE
- Grain refinement, APCs formation and enhanced J_c are consolidated material properties
- Significant progress is being made toward the development of scalable, application-ready wire fabrication methods that can reliably deliver these features

State-of-the-art Wire Properties

- The longitudinal strain state of the wire affects the magnet's operational margin and must be carefully considered during design
- In our experiments under transverse compression up to ~ 200 MPa, permanent degradation of state-of-the-art RRP wires is primarily driven by residual stresses



Swiss National
Science Foundation



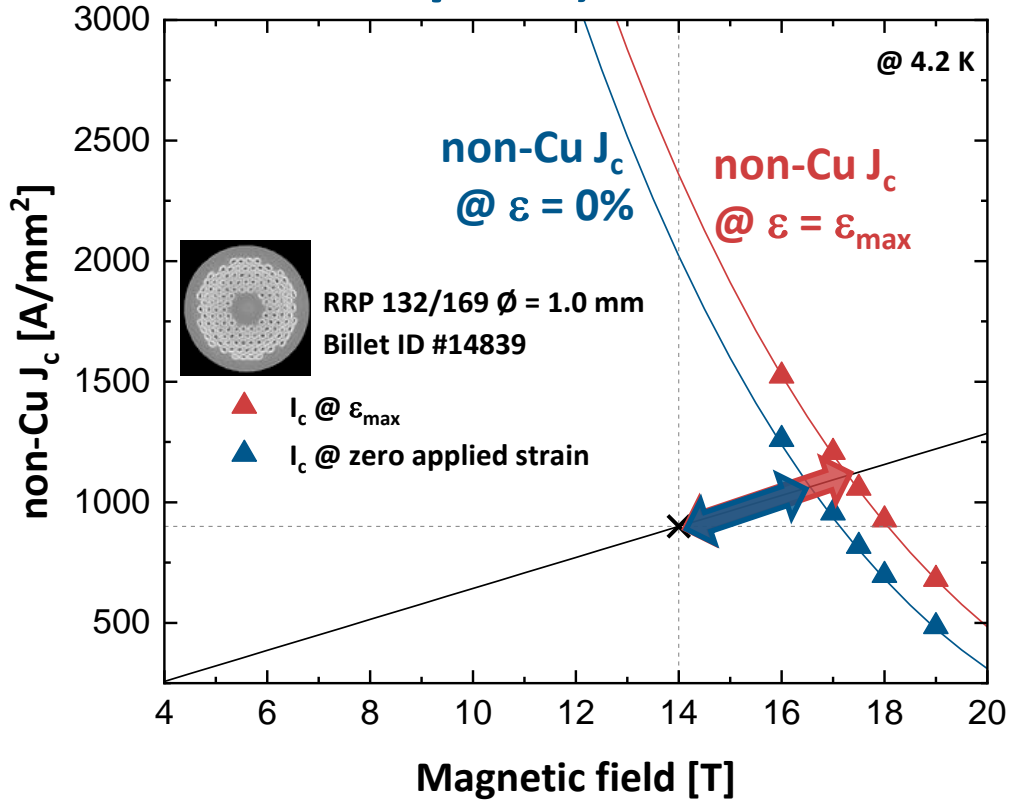
Thank you for the attention !

Carmine SENATORE
carmine.senatore@unige.ch
<http://supra.unige.ch>

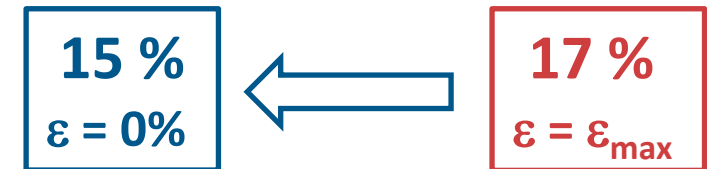
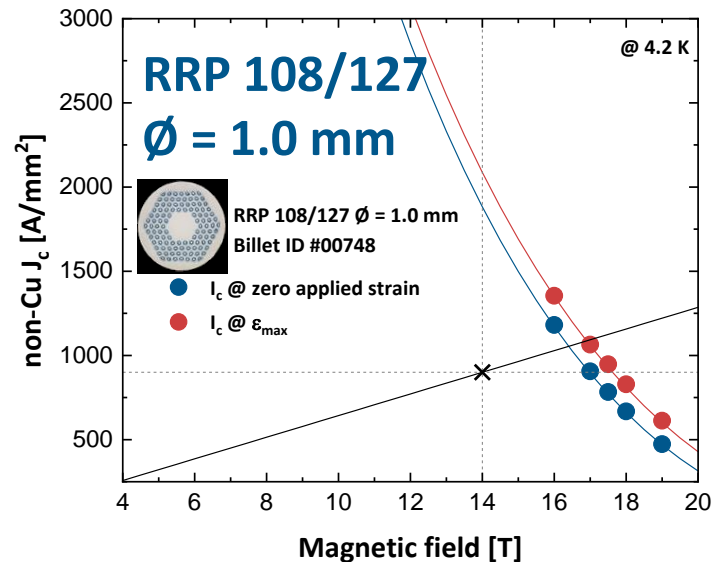
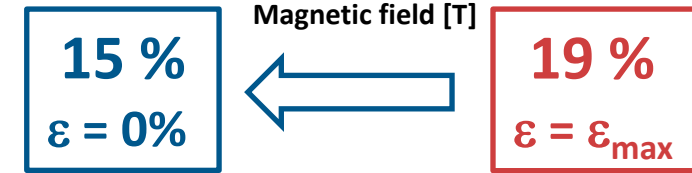
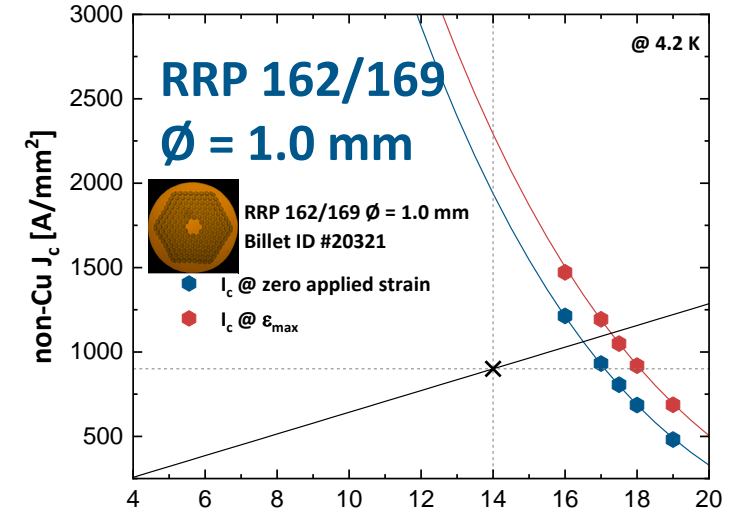
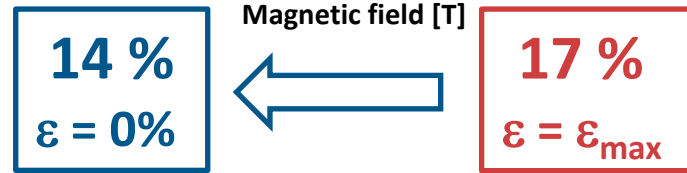
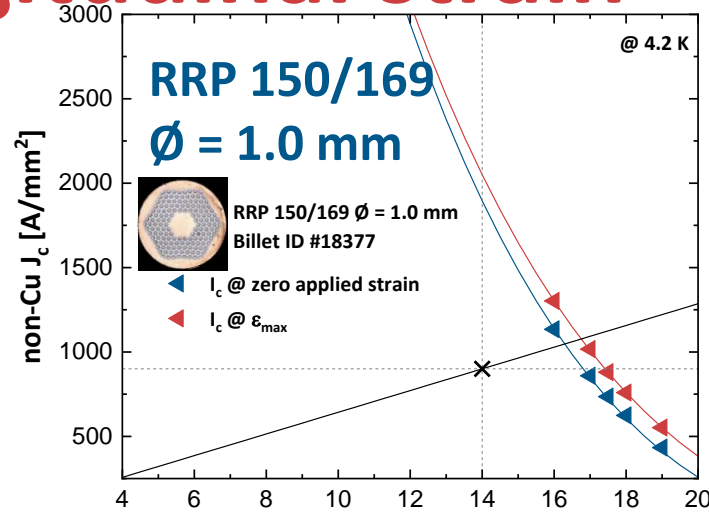
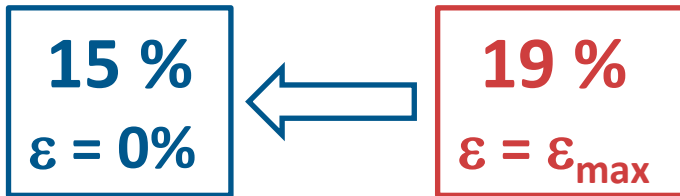
Acknowledgments: This work was done under the auspices of CHART (Swiss Accelerator Research and Technology Collaboration, <https://chart.ch>). Financial support was provided by the Swiss National Science Foundation (Grant No. 200021_184940), by the European Organization for Nuclear Research (CERN), Memorandum of Understanding for the FCC Study, Addendum FCC-GOV-CC-0175 (KE 4663/ATS).

Loadline margin vs longitudinal strain

RRP 132/169, $\phi = 1.0$ mm



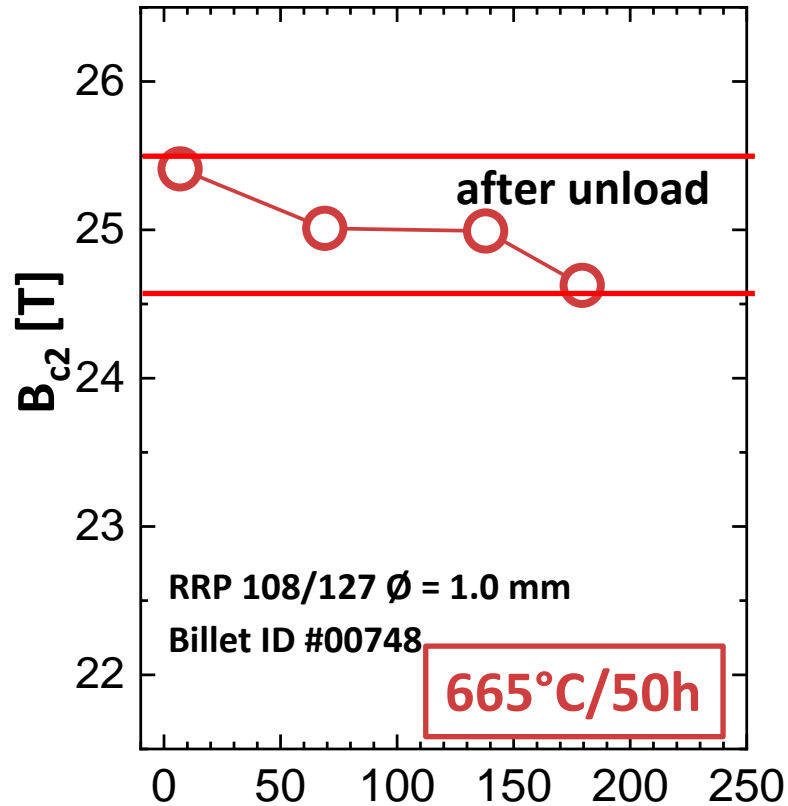
Loadline margin @ $T_{op} = 4.2$ K



Comparison of B_{c2} after unload, different wire diameters

(as determined from Kramer extrapolation)

108/127, $\phi = 1.0$ mm

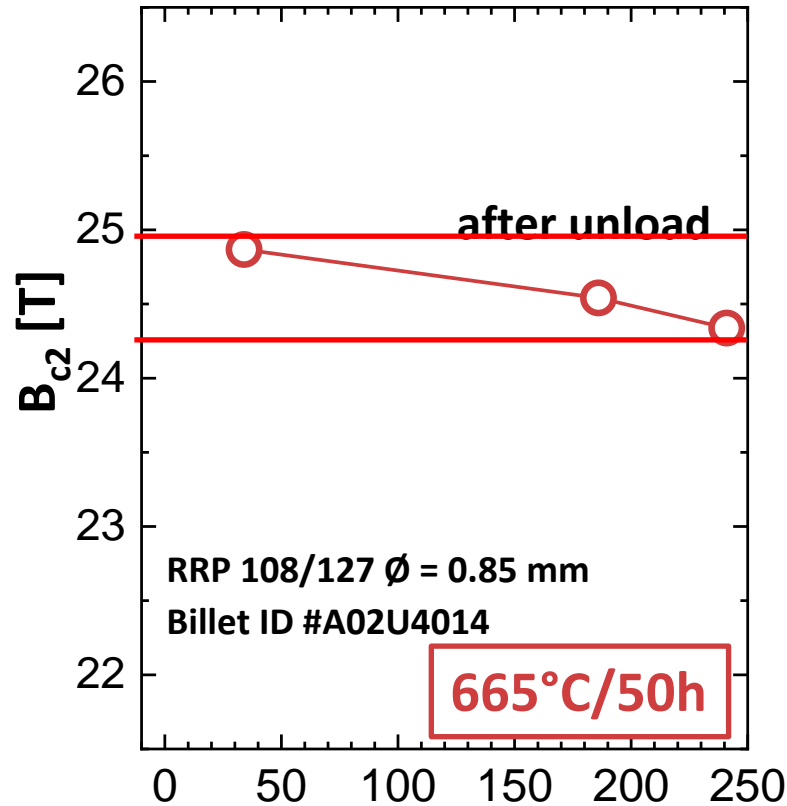


Transverse stress [MPa]

After unload from $\sigma = 180$ MPa

$$\Delta B_{c2}^{\text{unload}} \approx 0.8 \text{ T}$$

108/127, $\phi = 0.85$ mm

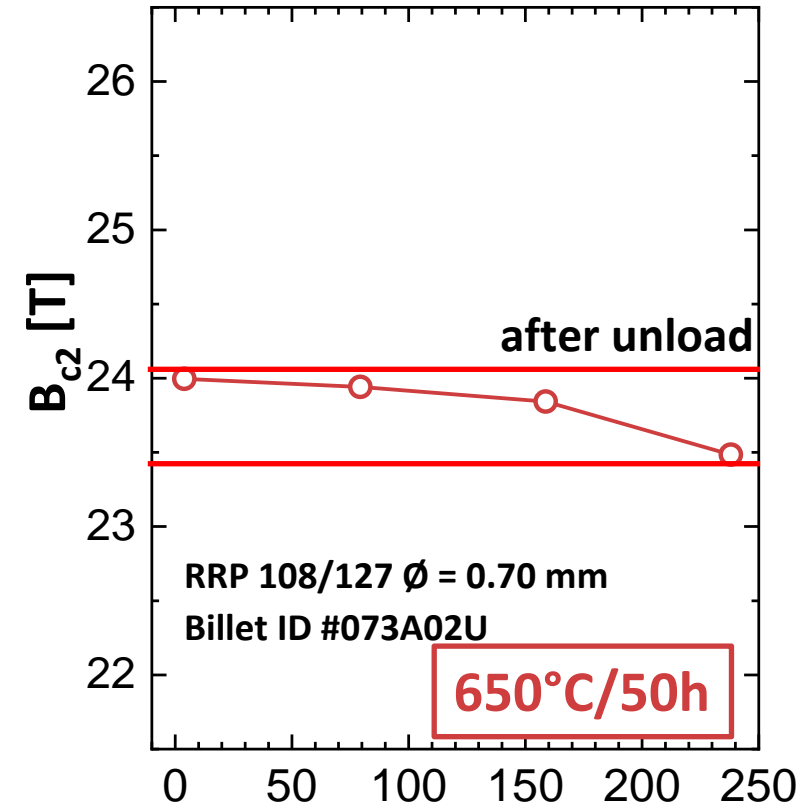


Transverse stress [MPa]

After unload from $\sigma = 240$ MPa

$$\Delta B_{c2}^{\text{unload}} \approx 0.5 \text{ T}$$

108/127, $\phi = 0.7$ mm



Transverse stress [MPa]

After unload from $\sigma = 240$ MPa

$$\Delta B_{c2}^{\text{unload}} \approx 0.5 \text{ T}$$

